Supporting Information

Triazonine-Based Bistable Photoswitches: Synthesis, Characterization and Photochromic Properties

Nawel Goual,[a‡] Lorenzo Casimiro,[b‡] Vincent Delattre,[a] Pascal Retailleau,[a] Stéphane Maisonneuve,[b] Nicolas Bogliotti,[b] Rémi Métivier,[b] Juan Xie,*[b] Angela Marinetti*[a] and Arnaud Voituriez*[a]

[a]Université Paris-Saclay, CNRS, Institut de Chimie des Substances Naturelles, UPR 2301, 91198, Gif-sur-Yvette, France. E-mails: arnaud.voituriez@cnrs.fr and angela.marinetti@cnrs.fr

[b]Université Paris-Saclay, ENS Paris-Saclay, CNRS, PPSM, 91190, Gif-sur-Yvette, France.
E-mail: joanne.xie@ens-paris-saclay.fr

[‡]These authors contributed equally.

Table of Contents:

I. General information.

Reactions were performed using oven dried glassware under an atmosphere of argon. All separations were carried out under flash-chromatographic conditions on silica gel (Redi Sep prepacked column, 230–400 mesh) at medium pressure (20 psi) with use of a CombiFlash Companion or preparative HPLC. Reactions were monitored by thin-layer chromatography on Merck silica gel plates (60 F254 aluminum sheets) which were rendered visible by ultraviolet and spraying with $KMnO_4$ solution (1.5 g of $KMnO_4$, 10 g K_2CO_3, and 1.25 mL 10% NaOH in 200 mL water), followed by heating. Reagent-grade chemicals were obtained from diverse commercial suppliers and used as received. ^1H NMR (500 or 300 MHz) and ^{13}C NMR (125 or 75 MHz) spectra were recorded on Brüker Avance spectrometers at 298 K unless otherwise stated. Chemical shifts are given in ppm (δ) and are referenced to the internal solvent signal. Multiplicities are declared as follow: s (singlet), bs (broad singlet), d (doublet), t (triplet), q (quadruplet), dd (doublet of doublet), m (multiplet). Coupling constants J are given in Hz. Carbon multiplicities were determined by DEPT135 experiment. Infrared spectra (IR) were recorded on a Perkin-Elmer FT-IR system using diamond window Dura SamplIR II and the data are reported in reciprocal centimeters (cm^{-1}). Melting points were recorded in open capillary tubes on a Büchi B-540 apparatus and are uncorrected. High-resolution mass spectrometry (HRMS) was performed using electrospray ionization (ESI) and time-of-flight (TOF) analyzer, in positive-ion or negative-ion detection mode.

II. Experimental procedures.

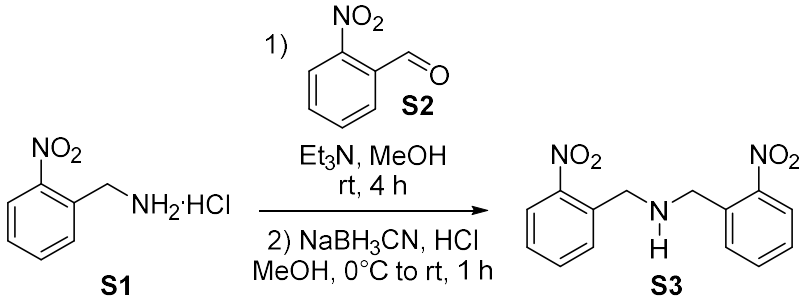

II.1. Bis(2-nitrobenzyl)amine (S3). 2-Nitrobenzenemethanamine hydrochloride **S1** (2.5 g, 13.25 mmol, 1 equiv.) was dissolved in MeOH (50 mL). Triethylamine (3.9 mL, 26.5 mmol, 2 equiv.) was added to the solution and the mixture was stirred at room temperature for 5 min. 2-Nitrobenzaldehyde **S2** (1.9 g, 12.6 mmol, 0.95 equiv.) was added in one portion in the flask. The stirring is maintained at rt until the imine precipitates. The solid was filtered and dissolved in MeOH (50 mL). The reaction was cooled to 0 °C and $NaBH_3CN$ (1.9 g, 12.6 mmol, 1.1 equiv.) was added in one portion. HCl aqueous solution (1M) was added and the reaction was stopped after 1 h at rt. The solvent is directly removed in vacuo. The crude was dissolved in EtOAc and water was added. The organic phase was then washed twice with $NaHCO_3$ sat., followed by NaCl sat. aqueous solution. The organic phases were collected and dried over $MgSO_4$, filtered and concentrated in vacuo. The pure product **S3** was obtained without further purification as a yellow solid (2.1 g, 75% yield). R_f 0.42 (10% EtOAc in Petroleum ether); mp 100−102 °C; ^{1}H NMR ($CDCl_3$, 300 MHz) δ 7.95 (dd, J = 8.4, 0.9 Hz, 2H), 7.65 – 7.54 (m, 4H), 7.46 – 7.38 (m, 2H), 4.08 (s, 4H), 2.14 (br, 1H); ^{13}C NMR ($CDCl_3$, 75 MHz) δ 149.3 (C), 135.3 (C), 133.3 (CH), 131.3 (CH), 128.3 (CH), 124.9 (CH), 50.5 (CH_2); IR (neat) ν_{max} = 2912, 2839, 1610, 1575, 1530, 1512, 1447, 1335, 1322, 1299, 1116, 1073, 863, 788, 723 cm^{-1}; HRMS (ESI) calcd. for $C_{14}H_{14}N_3O_4$ $[M+H]^+$: 288.0984, found: 288.0980.

II.2. *Tert*-butyl bis(2-nitrobenzyl)carbamate (1a). Bis(2-nitrobenzyl)amine **S3** (1 g, 3.48 mmol, 1 equiv.) was dissolved in dry dichloromethane (9 mL) and triethylamine (0.95 mL, 13.92 mmol, 4 equiv.) was added. A solution of Boc_2O (1.52 g, 6.96 mmol, 2 equiv.) in dry CH_2Cl_2 (9 mL) was added dropwise at 0°C. The reaction was maintained under stirring at room temperature overnight. The reaction was then quenched by the addition of water and extracted twice with dichloromethane. The organic layers were dried over $MgSO_4$ and filtered. The crude was purified by flash chromatography (10% EtOAc in

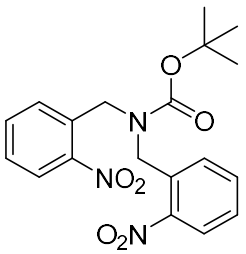

Petroleum ether) to give compound **1a** as a pale yellow solid (1.1 g, 82 % yield). R_f 0.27 (10% EtOAc in Petroleum ether); mp 108−110 °C; ^{1}H NMR ($CDCl_3$, 500 MHz) δ 8.05 (d, J = 7.8 Hz, 2H), 7.67 (td, J = 7.8, 1.2 Hz, 2H), 7.50 – 7.40 (m, 4H), 4.90 − 4.80 (m, 4H), 1.41 (s, 9H); ^{13}C NMR ($CDCl_3$, 75 MHz) δ 156.0 (C), 134.1 (CH), 128.3 (CH), 128.0 (CH), 125.5 (CH), 81.4 (C), 48.8 (CH_2), 48.5 (CH_2), 28.3 (CH_3); IR (neat) ν_{max} = 2976, 2902, 1695, 1522, 1452, 1357, 1339, 1275, 1251, 1162, 1126, 895, 857, 789, 729 cm^{-1}; HRMS (ESI) calcd. for $C_{21}H_{24}N_4NaO_6$ $[M+CH_3CN+Na]^+$: 451.1594, found: 451.1575.

II.3. Benzyl bis(2-nitrobenzyl)carbamate (1b). Bis(2-nitrobenzyl)amine **S3** (30 mg, 0.1 mmol, 1 equiv.) was dissolved in dry dichloromethane (1 mL) and triethylamine (42 µL, 0.3 mmol, 3 equiv.) was added. A solution of benzyl carbonochloridate (23 µL, 0.16 mmol, 1.5 equiv.) in dry CH_2Cl_2 (1 mL) was added dropwise at 0°C. The reaction was maintained under stirring at room temperature overnight. The reaction was then quenched by the addition of water and extracted twice with dichloromethane. The organic layers were dried over $MgSO_4$ and filtered. The crude was purified by flash chromatography (10% EtOAc in Petroleum ether) to give compound **1b** as a off-white solid (27 mg, 64 % yield). R_f 0.15 (10% EtOAc in Petroleum ether); mp 140–142 °C; ^{1}H NMR ($CDCl_3$, 500 MHz) δ 8.06 (bs, 2H), 7.68 – 7.55 (m, 2H), 7.45 (t, J = 7.5 Hz, 3H), 7.38 – 7.33 (m, 1H), 7.32 – 7.28 (m, 3H), 7.24 – 7.19 (m, 2H), 5.19 (s, 2H), 4.94 (s, 2H) 4.93 (s, 2H); ^{13}C NMR ($CDCl_3$, 75 MHz) δ 156.9 (C), 136.1 (C), 134.1 (CH), 128.6 (CH), 128.42 (CH), 128.40 (CH), 128.2 (CH), 127.9 (CH), 127.1 (C), 125.5 (CH), 68.1 (CH_2), 48.8 (CH_2); IR (neat) ν_{max} = 2958, 1703, 1530, 1457, 1409, 1339, 1304, 1269, 1246, 1118, 857, 789, 728, 650 cm^{-1}; HRMS (ESI) calcd. for $C_{22}H_{20}N_3O_6$ $[M+H]^+$: 422.1352, found: 422.1348.

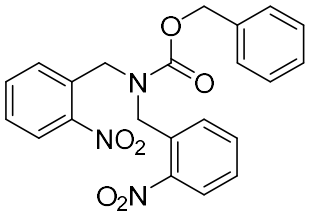

II.4. Ethyl bis(2-nitrobenzyl)carbamate (1c). Bis(2-nitrobenzyl)amine **S3** (500 mg, 1.74 mmol, 1 equiv.) was dissolved in dry dichloromethane (18 mL) and triethylamine (350 µL, 2.61 mmol, 1.5 equiv.) was added. Ethyl chloroformate (143 µL, 2.61 mmol, 1.5 equiv.) was added dropwise at 0°C. The reaction was maintained under stirring at room temperature 24 hrs. The reaction was then quenched by the addition of water and extracted twice with dichloromethane. The organic layers were dried over $MgSO_4$ and filtered. The crude was purified by flash chromatography (10% EtOAc in Petroleum ether) to give compound **1c** as an oil (420 mg, 67 % yield). R_f 0.35 (20%

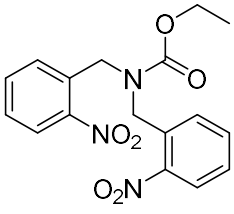

EtOAc in Petroleum ether); ^{1}H NMR ($CDCl_3$, 500 MHz) δ 8.06 (bs, 2H), 7.66 (td, J = 7.3 Hz, J = 1.3 Hz, 2H), 7.52 – 7.37 (m, 4H), 4.90 (s, 4H), 4.21 (q, J = 7.2 Hz, 2H) 1.21 (t, J = 7.2 Hz, 3H); ^{13}C NMR ($CDCl_3$, 75 MHz) δ 157.1 (C), 148.3 (C), 148.2 (C), 134.1 (CH), 133.5 (C), 133.2 (C), 128.4 (CH), 127.8 (CH), 125.5 (CH), 62.5 (CH_2), 48.6 (CH_2), 14.7 (CH_3); HRMS (ESI) calcd. for $C_{17}H_{18}N_3O_6$ $[M+H]^+$: 360.1196, found: 360.1157.

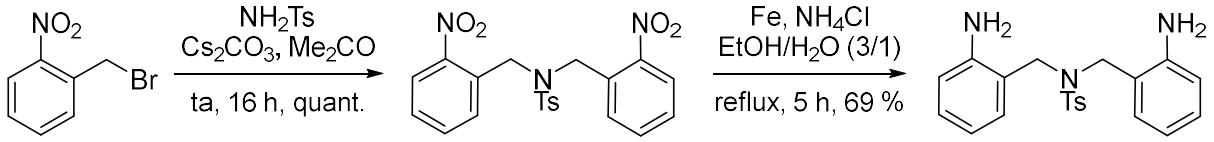

S4 **1d** **3**

II.5. 4-Methyl-*N*,*N*-bis(2-nitrobenzyl)benzenesulfonamide (1d). 1-(Bromomethyl)-2-nitrobenzene **S4** (1g, 3.08 mmol, 2.1 equiv.), *p*-toluenesulfonamide (260 mg, 1.43 mmol, 1 equiv.) and cesium carbonate (1.5 g, 4.62 mmol, 3 equiv.) were introduced in a flask. Acetone (6 mL) was added and the reaction was stirred at room temperature for 16 h. The mixture was filtered and concentrated. The crude mixture was dissolved in dichloromethane and washed with water. The organic phase was extracted with dichloromethane, dried over $MgSO_4$ and filtered. The crude mixture was purified by flash chromatography (5% to 30% EtOAc in Petroleum ether) to give product **2d** as a beige solid (635 mg, 99 % yield). R_f 0.25 (10% EtOAc in Petroleum ether); mp 164–167 °C; ^{1}H NMR ($CDCl_3$, 500 MHz) δ 7.81 (dd, J = 8.2, 1.1 Hz, 2H), 7.74 (t, J = 8.2 Hz, 2H), 7.54 (d, J = 7.5 Hz, 2H), 7.45 (td, J = 7.6, 1.1 Hz, 2H), 7.35 (d, J = 8.0 Hz, 2H), 7.31 (td, J = 7.6, 1.5, 2H), 4.80 (s, 4H), 2.47 (s, 3H); ^{13}C NMR ($CDCl_3$, 75 MHz) δ 148.4 (C), 144.4 (C), 136.2 (C), 133.5 (CH), 131.8 (C), 130.6 (CH), 130.2 (CH), 128.6 (CH), 127.4 (CH), 124.9 (CH), 50.0 (CH_2), 21.7 (CH_3); IR (neat) ν_{max} = 2925, 1523, 1342, 1306, 1159, 1094, 859, 786, 729, 657 cm^{-1}; HRMS (ESI) calcd. for $C_{21}H_{20}N_3O_6S$ $[M+H]^+$: 442.1073, found: 442.1085.

II.6. *N*,*N*-bis(2-aminobenzyl)-4-methylbenzenesulfonamide (3). 2d (100 mg, 0.26 mmol, 1 equiv.) was dissolved in absolute ethanol (0.087 mol/L) and a solution of NH_4Cl (70 mg, 1.3 mmol, 5 equiv.) in distilled water (1.3 mol/L) was added to the mixture. Iron (106 mg, 1.9 mmol, 7.2 equiv.) was added and the reaction was refluxed until completion (5 hrs). After cooling to rt, the mixture was filtered and concentrated. The crude was dissolved with EtOAc and washed three times with water and brine. The organic layers were dried over $MgSO_4$. The pure product **3** was obtained without any purification (60 mg, 69%). R_f 0.35 (20% EtOAc in Petroleum ether); mp 159–163 °C; ^{1}H NMR ($CDCl_3$, 300 MHz) δ 7.75 (d, J = 7.8 Hz, 2H),

7.35 (d, J = 7.8 Hz, 2H), 6.97 (t, J = 7.3 Hz, 2H), 6.70 (d, J = 7.3 Hz, 2H), 6.52-6.44 (m, 4H), 4.18 (s, 4H), 4.20-4.10 (bs, 4H), 2.47 (s, 3H); ^{13}C NMR ($CDCl_3$, 75 MHz) δ 146.3 (C), 144.1 (C), 134.4 (C), 131.2 (CH), 130.0 (CH), 129.3 (CH), 127.9 (CH), 118.8 (C), 117.7 (CH), 115.9 (CH), 51.3 (CH_2), 21.7 (CH_3); IR (neat) ν_{max} = 3469, 3382, 2924, 2854, 1630, 1496, 1332, 1314, 1159, 1091, 908, 749, 730, 711, 658 cm^{-1}; HRMS (ESI) calcd. for $C_{21}H_{24}N_3O_6S$ $[M+H]^+$: 382.1589, found: 382.1581.

General Procedure for the reductive cyclization of 2,2'-dinitrodibenzyls 1a-d:

Bis-nitrobenzene derivative **1a-d** (1 equiv.) was dissolved in absolute ethanol (0.02 mol/L) and heated at 70 °C in the dark. A hot solution of barium hydroxide (3 equiv.) in distilled water (0.11 mol/L) and activated zinc dust (16 equiv.) were introduced and the heating is pursued for 72 h. The mixture was cooled to room temperature and filtered on celite. The filtrate was concentrated in vacuo and the resulting crude mixture was dissolved in a 0.1 M NaOH methanolic solution (0.0148 mol/L). $CuCl_2$ (4 mol%) was added and air was bubbled in the solution for additional three hours. After that the solution was acidified with a 1 M HCl aqueous solution, followed by a $NaHCO_3$ sat. aqueous solution. The organic layers were extracted with dichloromethane and washed with brine. The organic layers were dried over $MgSO_4$ and filtered.

II.7. *Tert*-butyl (*E*)-11,13-dihydro-12*H*-dibenzo[*c*,*h*][1,2,6]triazonine-12-carboxylate (*E*-2a). Starting from *tert*-butyl bis(2-nitrobenzyl)carbamate **1a** (1 g, 2.28 mmol, 1 equiv.) and following the *General Procedure*, the resulting crude mixture was purified by flash chromatography (5 to 10% EtOAc in Petroleum ether) to furnish the pure (*E*)-isomer as an orange solid (300 mg, 36% yield). R_f 0.34 (10% EtOAc in Petroleum ether); mp 100-103 °C; ^{1}H NMR ($CDCl_3$, 500 MHz) δ 7.64 (dd, J = 7.9, 0.8 Hz, 1H), 7.50 – 7.37 (m, 4H), 7.37 – 7.31 (m, 2H), 7.30 – 7.27 (m, 1H), 4.60 (s, 4H), 1.02 (s, 9H); ^{13}C NMR ($CDCl_3$, 75 MHz) δ 154.9 (C), 154.5 (C), 154.3 (C), 131.8 (C), 131.5 (C), 130.0 (CH), 129.1 (CH), 128.7 (CH), 128.3 (CH),128.0 (CH), 122.2 (CH), 119.0 (CH), 79.9 (C), 57.8 (CH_2), 57.1 (CH_2), 28.2 (CH_3); IR (neat) ν_{max} = 3676, 2973, 2902, 1664, 1459, 1403, 1394, 1366, 1249, 1075, 1066, 1057, 1028, 768 cm^{-1}; HRMS (ESI) calcd. for $C_{21}H_{24}N_4NaO_2$ $[M+CH_3CN+Na]^+$: 387.1797, found: 387.1785.

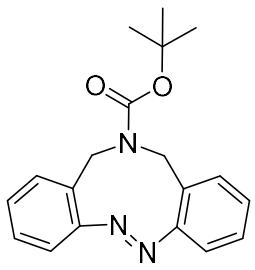

II.8. *Tert*-butyl (*Z*)-11,13-dihydro-12*H*-dibenzo[*c*,*h*][1,2,6]triazonine-12-carboxylate (*Z*-2a). The (*E*)-isomer can be isomerized into the pure (*Z*)-isomer at 334 nm and isolated as a yellow solid. R_f 0.58 (10% EtOAc in Petroleum ether); mp 128-130 °C; ^{1}H NMR ($CDCl_3$, 500 MHz) δ 7.48 (d, J = 8.0 Hz, 1H), 7.31 (d, J = 7.5 Hz, 1H), 7.15 – 7.10 (m, 2H), 7.02 – 6.95 (m, 2H), 6.47 (t, J = 7.5 Hz, 2H), 5.01 (d, J = 14.5 Hz, 1H), 4.84 (d, J = 15.0 Hz, 1H), 3.71 (d, J = 15.0 Hz, 1H), 5.57 (d, J = 14.0 Hz, 1H), 1.52 (s, 9H); ^{13}C NMR ($CDCl_3$, 75 MHz) δ 155.7 (C), 155.6 (C), 154.9 (C), 131.9 (CH), 130.8 (CH), 128.2 (CH), 128.0 (CH), 127.1 (CH), 126.9 (CH), 124.9 (C), 124.8 (C), 117.6 (CH), 117.2 (CH), 80.7 (C), 47.4 (CH_2), 47.0 (CH_2), 28.7 (CH_3); IR (neat) ν_{max} = 2974, 2930, 1688, 1456, 1411, 1366, 1239, 1155, 1118, 882, 867, 766, 758, 738, 676 cm^{-1}; HRMS (ESI) calcd. for $C_{21}H_{24}N_4NaO_2$ $[M+CH_3CN+Na]^+$: 387.1797, found: 387.1775.

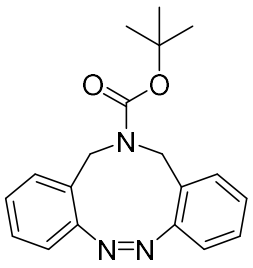

II.9. Benzyl (*E*)-11,13-dihydro-12*H*-dibenzo[*c*,*h*][1,2,6]triazonine-12-carboxylate (*E*-2b). Starting from benzyl bis(2-nitrobenzyl)carbamate **1b** (120 mg, 0.28 mmol, 1 equiv.) and following the *General Procedure*, the resulting crude mixture was purified by flash chromatography (5 to 10% EtOAc in Petroleum ether) to furnish the pure (*E*)-isomer as an orange solid (34 mg, 34 %). R_f 0.20 (10% EtOAc in Petroleum ether); mp 149–151 °C; ^{1}H NMR ($CDCl_3$, 500 MHz) δ 7.64 (dd, J = 7.8, 1.2 Hz, 1H), 7.53 – 7.41 (m, 4H), 7.36 (td, J = 7.7, 1.5 Hz, 1H), 7.29 (td, J = 7.8, 1.1 Hz, 1H), 7.24 – 7.20 (m, 1H), 7.20 – 7.13 (m, 3H), 6.85 – 6.78 (m, 2H), 4.77 (s, 2H), 4.69 (s, 2H), 4.68 (s, 2H); ^{13}C NMR ($CDCl_3$, 75 MHz) δ 155.4 (C), 154.7 (C), 136.5 (C), 131.2 (C), 130.8 (C), 129.9 (CH), 129.6 (CH), 128.8 (CH), 128.6 (CH), 128.4 (CH), 128.3 (CH), 128.2 (CH), 127.7 (CH), 127.4 (CH), 122.0 (CH), 119.8 (CH), 67.1 (CH_2), 57.8 (CH_2), 57.6 (CH_2); IR (neat) ν_{max} = 2988, 2971, 2923, 2902, 1698, 1473, 1451, 1409, 1273, 1245, 1130, 1076, 1066, 1057, 768, 732 cm^{-1}; HRMS (ESI) calcd. for $C_{22}H_{20}N_3O_2$ $[M+H]^+$: 358.1556, found: 358.1563.

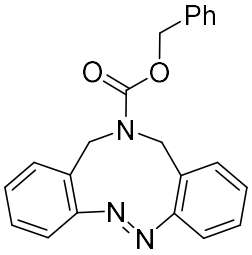

II.10. Benzyl (*Z*)-11,13-dihydro-12*H*-dibenzo[*c*,*h*][1,2,6]triazonine-12-carboxylate (*Z*-2b).

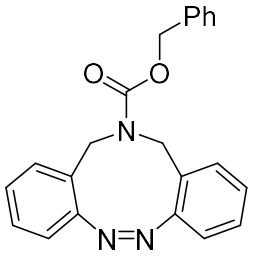

The pure (*E*) compound can be isomerized into the (Z) form at 334 nm and isolated as a yellow solid. R_f 0.35 (10% EtOAc in Petroleum ether); mp 124 – 127 °C; ^{1}H NMR ($CDCl_3$, 500 MHz) δ 7.51 (d, J = 7.5 Hz, 1H), 7.41 – 7.31 (m, 5H), 7.17 – 7.07 (m, 3H), 7.01 (t, J = 7.5 Hz, 1H), 6.89 (t, J = 8.0 Hz, 1H), 6.48 (d, J = 7.5 Hz, 1H), 6.46 (d, J = 7.5 Hz, 1H), 5.24 (d, J = 12.0 Hz, 1H), 5.14 (d, J = 12.0 Hz, 1H), 5.07 (d, J = 14.5 Hz, 1H), 4.90 (d, J = 15.0 Hz, 1H), 3.71 (d, J = 14.5 Hz, 1H), 3.63 (d, J = 14.5 Hz, 1H); ^{13}C NMR ($CDCl_3$, 75 MHz) δ 132.0 (CH), 131.2 (CH), 128.7 (CH), 128.4 (CH), 128.3 (CH), 127.2 (CH), 127.0 (CH), 124.4 (C), 124.3 (C), 117.5 (CH), 117.3 (CH), 67.9 (CH_2), 47.7 (CH_2), 47.2 (CH_2); IR (neat) ν_{max} = 2922, 2853, 1698, 1458, 1420, 1227, 1115, 766, 740, 698 cm^{-1}; HRMS (ESI) calcd. for $C_{22}H_{20}N_3O_2$ $[M+H]^+$: 358.1556, found: 358.1550.

II.11. *Tert*-butyl (*E*)-11,13-dihydro-12*H*-dibenzo[*c*,*h*][1,2,6]triazonine-12-carboxylate (*E*-2c). Starting from ethyl bis(2-nitrobenzyl)carbamate **1c** (400 mg, 1.11 mmol, 1 equiv.) and following the *General Procedure*, the resulting crude mixture was purified by flash chromatography (10 to 20% EtOAc in Petroleum ether). The isomeric ratio determined by ^{1}H NMR of the crude mixture was *E*/*Z* = 80/20. Pure (*Z*)-isomer was isolated as a yellow solid (32 mg, 10% yield) and (*E*)-isomer as an orange solid (137 mg, 42% yield). R_f 0.37 (20% EtOAc in Petroleum ether); mp 102-105 °C; ^{1}H NMR ($CDCl_3$, 300 MHz) δ 7.60 (dd, J = 7.6, 1.1 Hz, 1H), 7.54 – 7.34 (m, 4H), 7.39 – 7.27 (m, 3H), 4.66 (s, 2H), 4.64 (s, 2H), 3.76 (q, J = 7.2 Hz, 2H), 0.83 (t, J = 7.2 Hz, 3H); ^{13}C NMR ($CDCl_3$, 75 MHz) δ 155.5 (C), 154.6 (C), 154.4 (C), 131.2 (C), 131.1 (C), 129.6 (CH), 129.6 (CH), 128.8 (CH), 128.4 (CH), 128.3 (CH), 128.2 (CH), 121.4 (CH), 120.1 (CH), 61.1 (CH_2), 57.7 (CH_2), 57.4 (CH_2), 14.3 (CH_3) ; IR (neat) ν_{max} = 2977, 1698, 1461, 1408, 1274, 1244, 1126, 1028, 769, 735 cm^{-1}; HRMS (ESI) calcd. for $C_{17}H_{18}N_3O_2$ $[M+H]^+$: 296.1399, found: 296.1383.

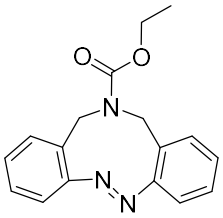

II.12. *Tert*-butyl (*E*)-11,13-dihydro-12*H*-dibenzo[*c*,*h*][1,2,6]triazonine-12-carboxylate (*Z*-2c). R_f 0.54 (20% EtOAc in Petroleum ether); mp 137-142 °C; ^{1}H NMR ($CDCl_3$, 500 MHz) δ 7.48 (d, J = 7.6 Hz, 1H), 7.30 (d, J = 7.6 Hz, 1H), 7.15 – 7.10 (m, 2H), 6.99 (td, J = 7.0 Hz, 1.0 Hz, 2H), 6.48 (d, J = 7.5 Hz, 2H), 5.05 (d, J = 14.3 Hz, 1H), 4.89 (d, J = 14.3 Hz, 1H), 4.24 – 4.19

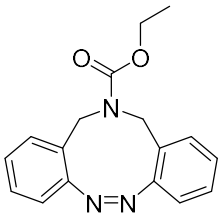

(m, 2H), 3.71 (d, J = 14.3 Hz, 1H), 3.61 (d, J = 14.3 Hz, 1H), 1.35 (t, J = 7.2 Hz, 3H); ^{13}C NMR ($CDCl_3$, 125 MHz) δ 155.9 (C), 155.6 (C), 132.0 (CH), 130.1 (CH), 129.6 (C), 128.4 (CH), 128.2 (CH), 127.1 (CH), 127.0 (CH), 124.6 (C), 124.5 (C), 117.5 (CH), 117.2 (CH), 61.9 (CH_2), 47.5 (CH_2), 47.1 (CH_2), 14.9 (CH_3); IR (neat) ν_{max} = 2929, 1691, 1458, 1421, 1302, 1270, 1229, 1117, 768, 740 cm^{-1}; HRMS (ESI) calcd. for $C_{17}H_{18}N_3O_2$ $[M+H]^+$: 296.1399, found: 296.1401.

II.13. (*E*)-12-tosyl-12,13-dihydro-11*H*-dibenzo[*c*,*h*][1,2,6]triazonine (*E*-4).

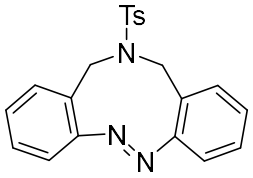

N,*N*-bis(2-aminobenzyl)-4-methylbenzenesulfonamide **3** (30 mg, 0.079 mmol, 1 equiv.) was dissolved in 2 mL of a mixture CH_2Cl_2 /AcOH (3/1) under inert atmosphere. A freshly prepared solution of *m*CPBA in glacial AcOH (27 mg, 1 equiv., 0.6 M) was added dropwise. After the addition, the reaction was stirred at room temperature 15 minutes and then heated at 80°C during 3 days. The reaction was then cooled to r.t. and concentrated under reduced pressure. The crude was dissolved in EtOAc and washed with a saturated solution of $NaHCO_3$ followed by brine. The organic layers were dried over $MgSO_4$ and filtered. The crude was purified by flash chromatography (8% of EtOAc in petroleum ether) to give the product as a *E*/*Z* mixture 90/10 (13 mg, 44% yield). R_f 0.34 (10% EtOAc in Petroleum ether); ^{1}H NMR ($CDCl_3$, 500 MHz) δ 7.47 – 7.41 (m, 2H), 7.40 – 7.37 (m, 2H), 7.36 – 7.33 (m, 4H), 6.78 (d, J = 8.0 Hz, 2H), 6.68 (d, J = 8.0 Hz, 2H), 4.80 (s, 4H), 2.24 (s, 3H); ^{13}C NMR ($CDCl_3$, 75 MHz) δ 154.3 (C), 142.6 (C), 136.2 (C), 130.0 (CH), 129.9 (C), 128.9 (CH), 128.8 (CH), 128.7 (CH), 126.9 (CH), 121.4 (CH), 58.6 (CH_2), 21.5 (CH_3); HRMS (ESI) calcd. for $C_{21}H_{20}N_3O_2S$ $[M+H]^+$: 387.1276, found: 387.1271.

II.14. (*Z*)-12-tosyl-12,13-dihydro-11*H*-dibenzo[*c*,*h*][1,2,6]triazonine (*Z*-4). Starting from the 90/10 : *E*/*Z* mixture, the ratio can be reversed to a 3/97 mixture (*E*)/(Z) after irradiation at 334 nm (yellow solid). R_f 0.34 (10% EtOAc in Petroleum ether); ^{1}H NMR ($CDCl_3$, 500 MHz) δ 7.72 (d, J = 8.0 Hz, 2H), 7.37 – 7.32 (m, 4H), 7.11 (td, J = 8.0, 1.5 Hz, 2H), 7.02 (td, J = 8.0, 1.0 Hz, 2H), 6.41 (d, J = 8.0 Hz, 2H), 4.72 (d, J = 14.3 Hz, 2H), 3.45 (d, J = 13.7 Hz, 2H), 2.45 (s, 3H); ^{13}C NMR ($CDCl_3$, 75 MHz) δ 155.9 (C), 143.8 (C), 136.8 (C), 131.9 (CH), 130.1 (CH), 128.6 (CH), 127.3 (CH), 127.1 (CH), 123.0 (C), 117.3 (CH), 49.1 (CH_2), 21.7 (CH_3); IR (neat) ν_{max} = 2924, 2855, 1445, 1336, 1159, 1089, 1048, 1033, 898, 806, 757, 742, 717, 655 cm^{-1}; HRMS (ESI) calcd. for $C_{21}H_{20}N_3O_2S$ $[M+H]^+$: 387.1276, found: 387.1262.

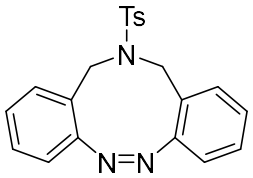

IV. NMR Spectra (^{1}H and ^{13}C NMR).

IV.1. Compound (S3).

^{1}H NMR ($CDCl_3$, 300 MHz)

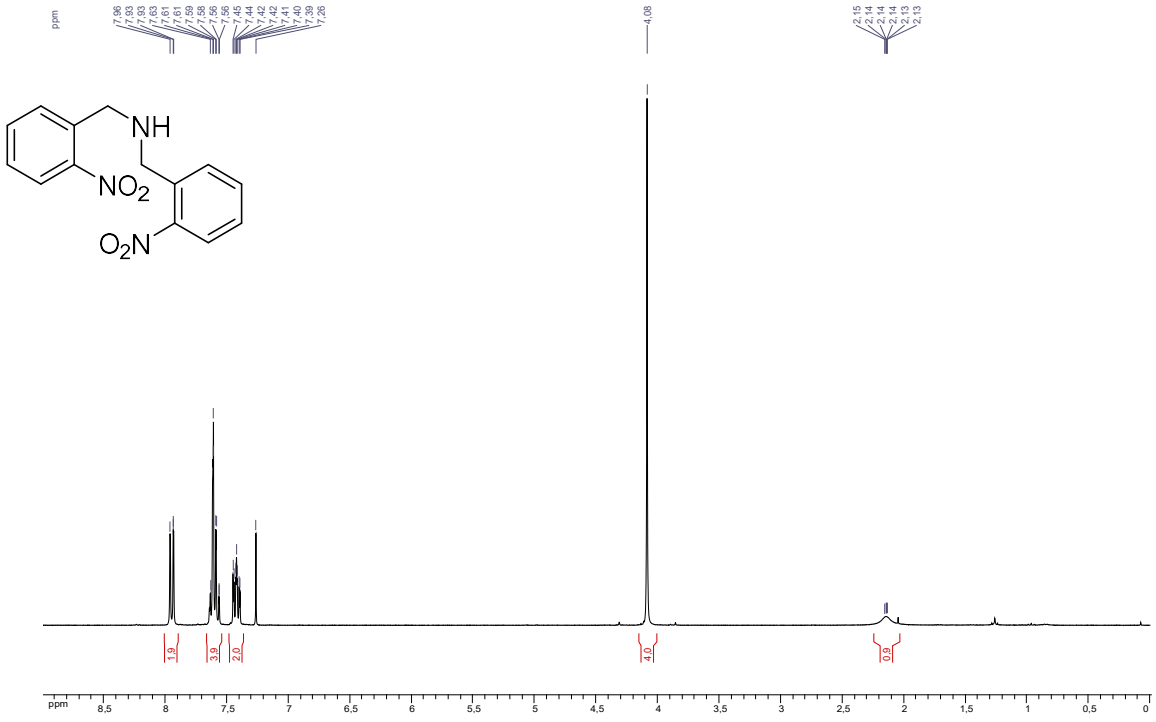

^{13}C NMR ($CDCl_3$, 75 MHz)

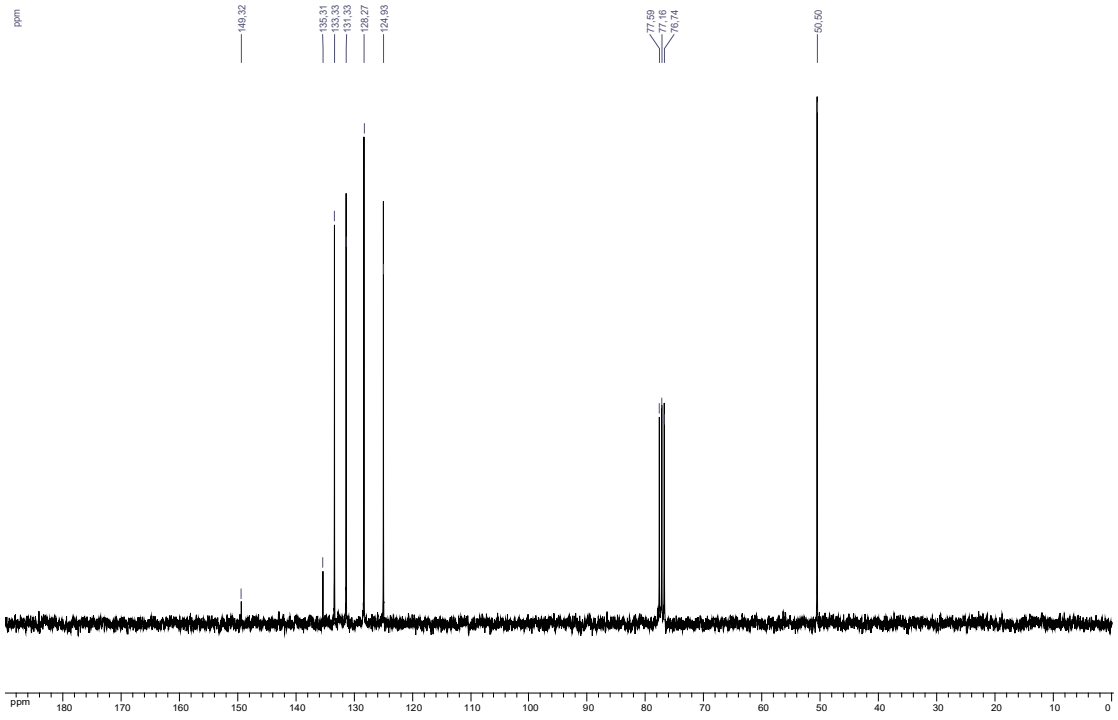

IV.2. Compound (1a).

^{1}H NMR ($CDCl_3$, 300 MHz)

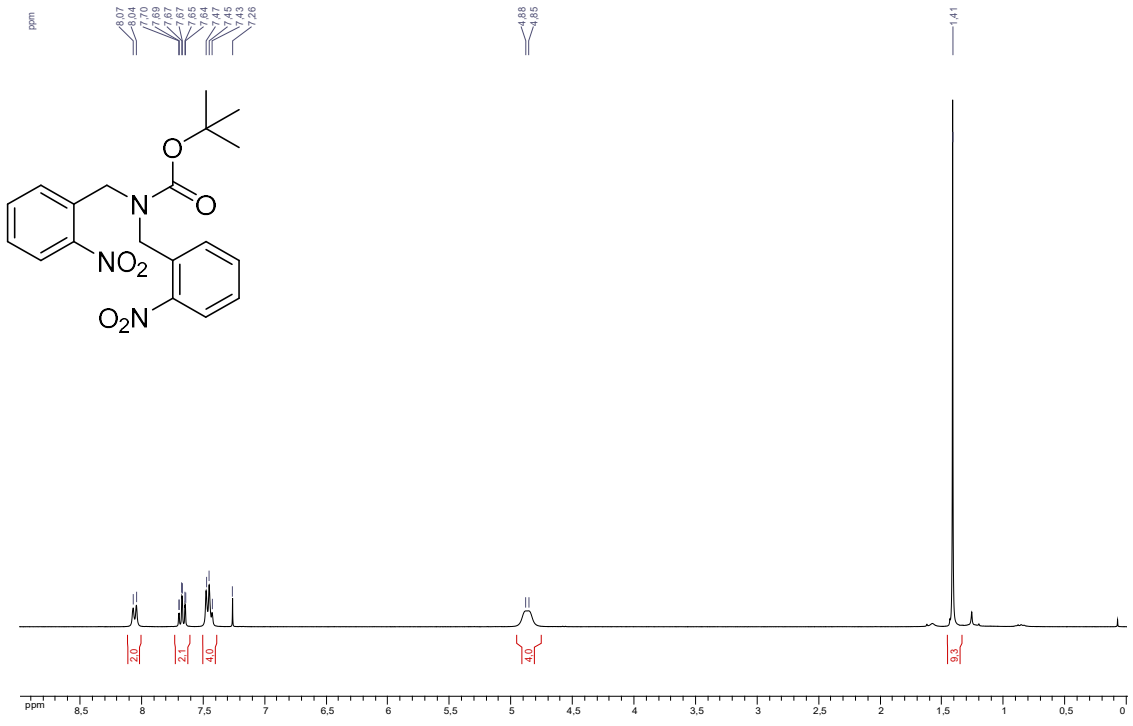

^{13}C NMR ($CDCl_3$, 75 MHz)

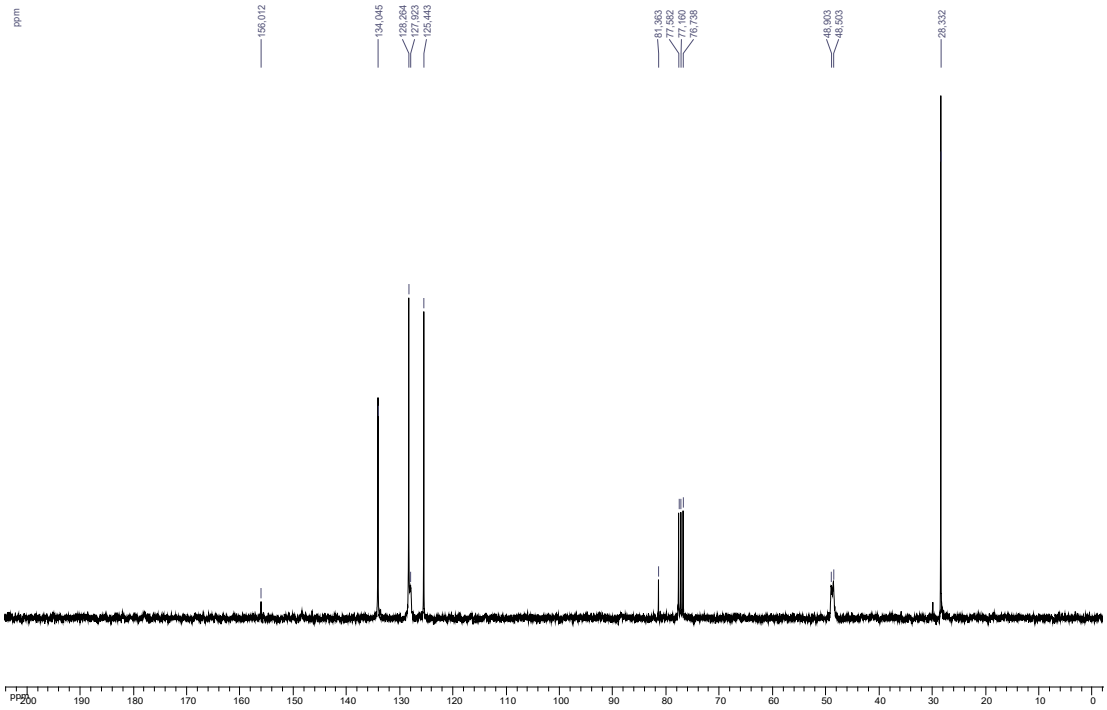

IV.3. Compound (1b).

^{1}H NMR ($CDCl_3$, 300 MHz)

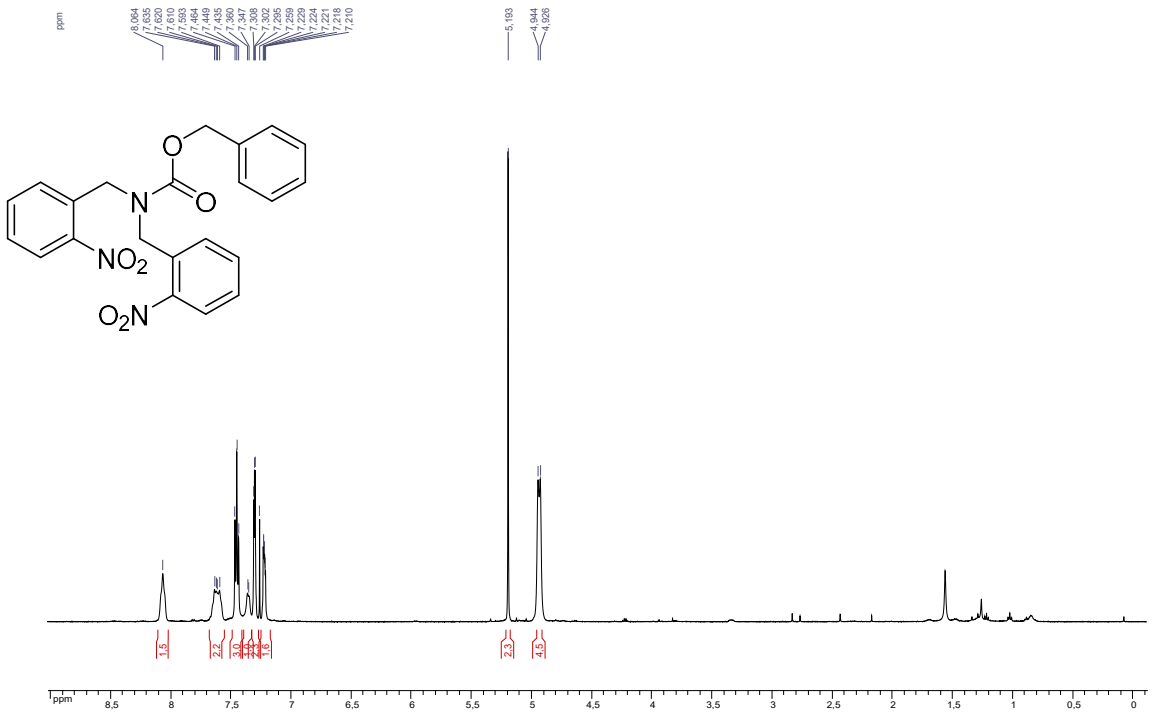

^{13}C NMR ($CDCl_3$, 75 MHz)

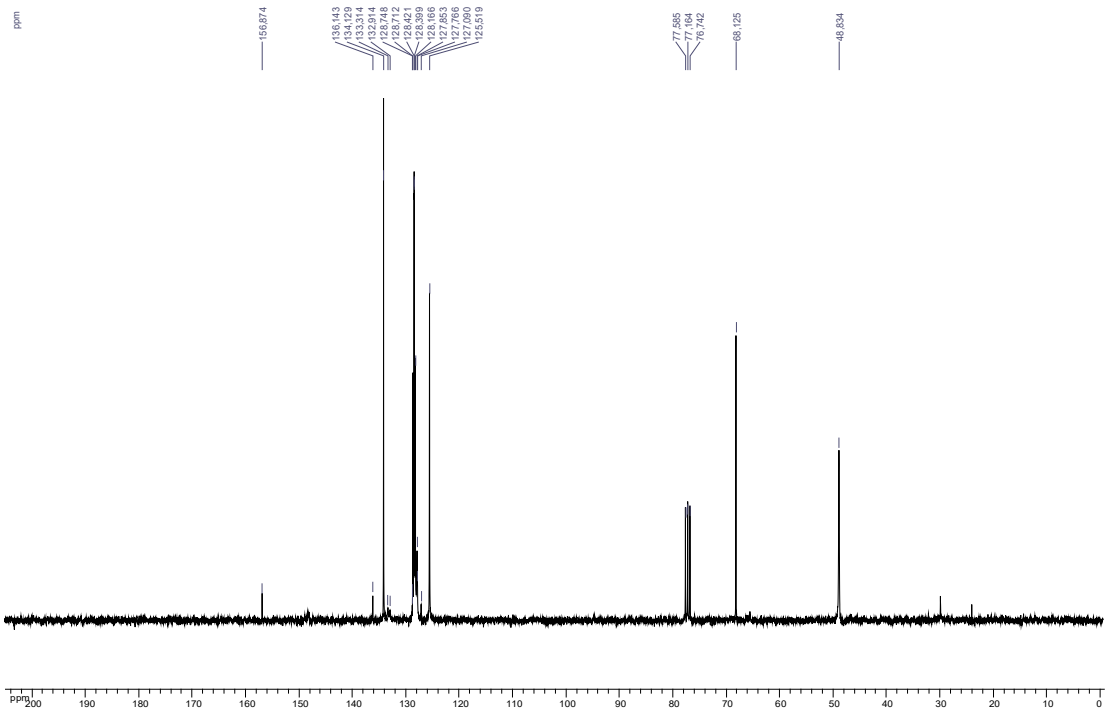

IV.4. Compound (1c).

^{1}H NMR ($CDCl_3$, 500 MHz)

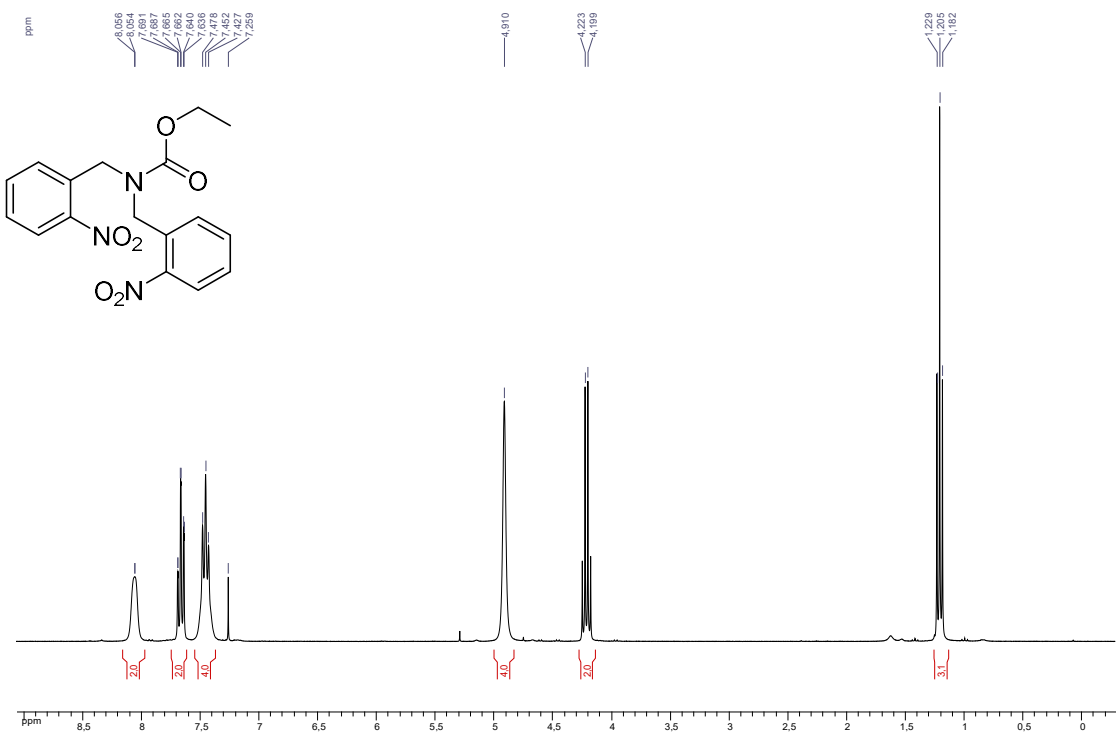

^{13}C NMR ($CDCl_3$, 75 MHz)

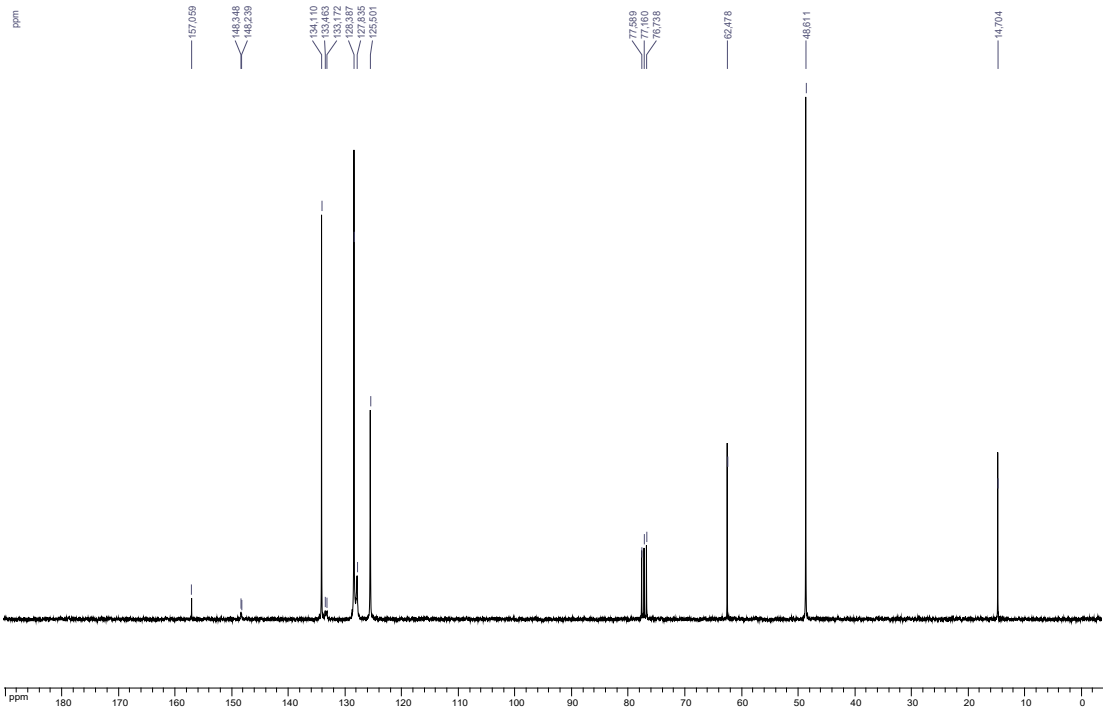

IV.5. Compound (1d).

^{1}H NMR ($CDCl_3$, 500 MHz)

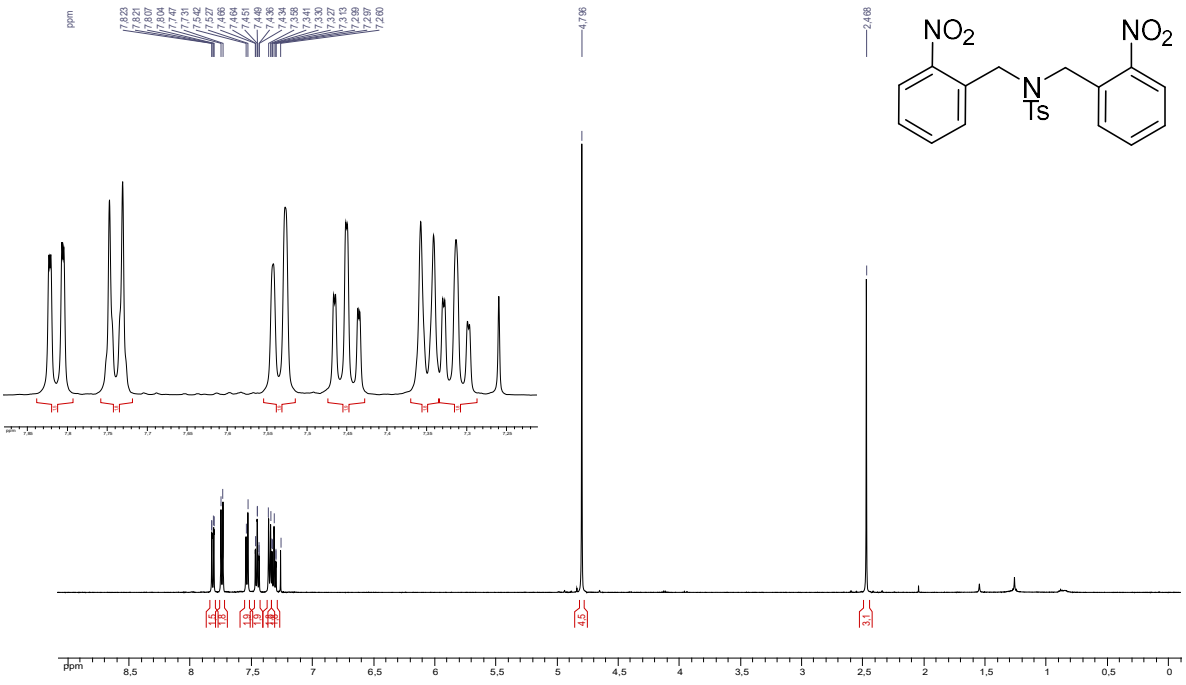

^{13}C NMR ($CDCl_3$, 75 MHz)

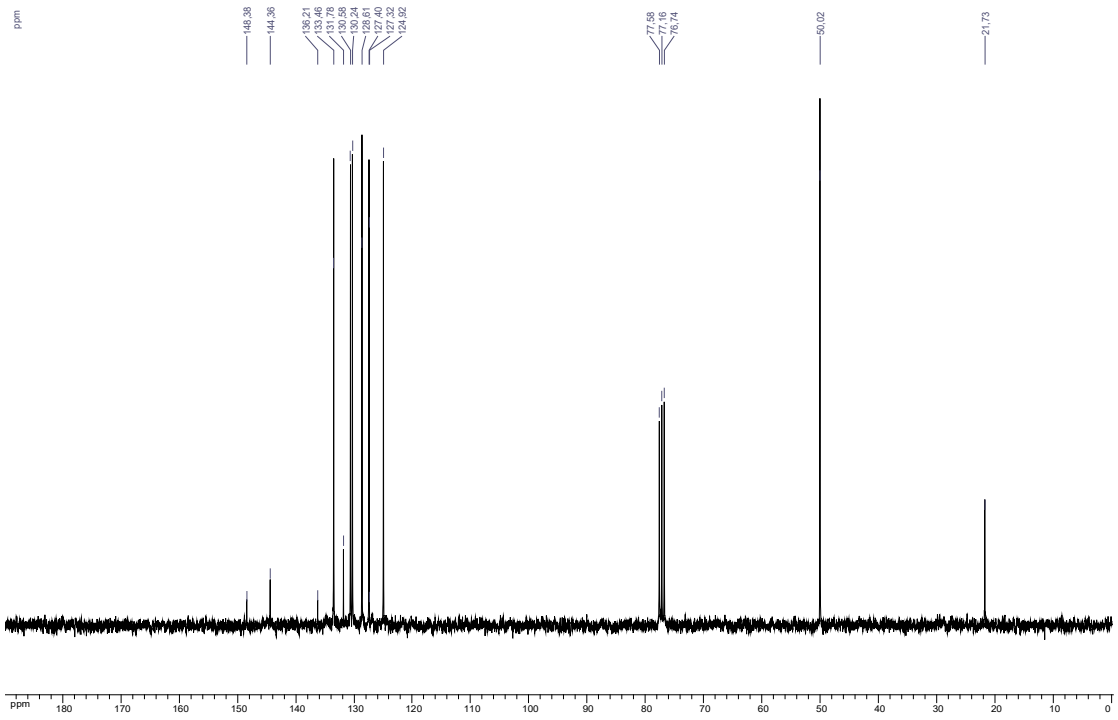

IV.6. Compound (3).

^{1}H NMR ($CDCl_3$, 500 MHz)

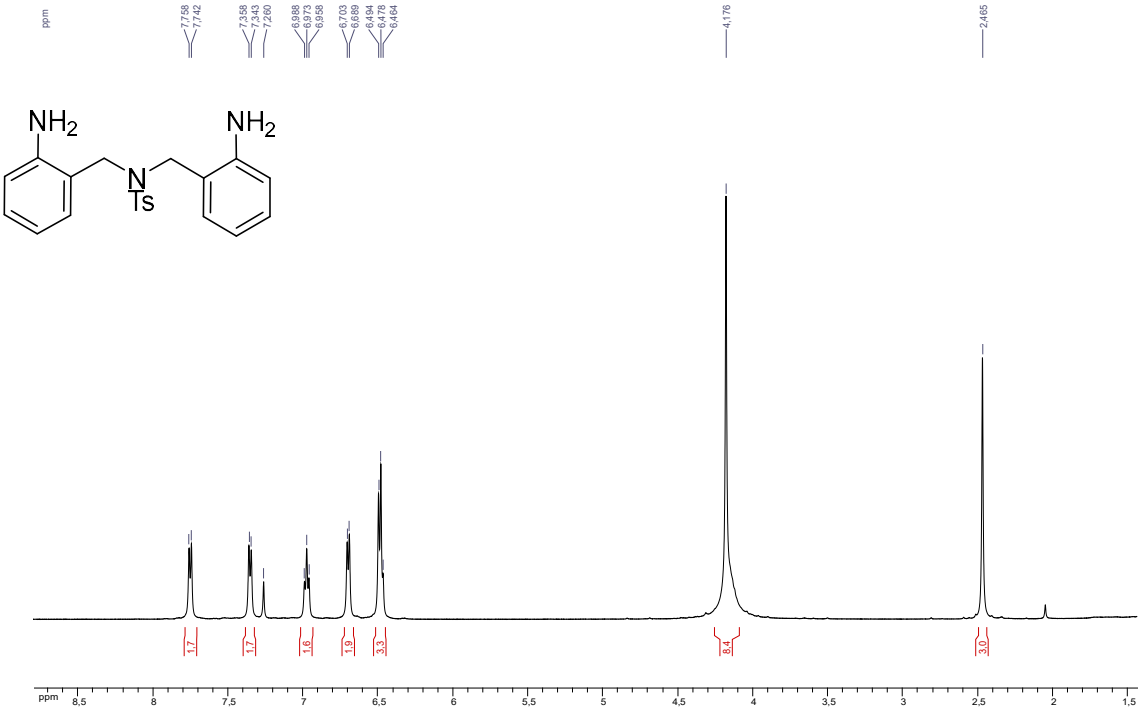

^{13}C NMR ($CDCl_3$, 75 MHz)

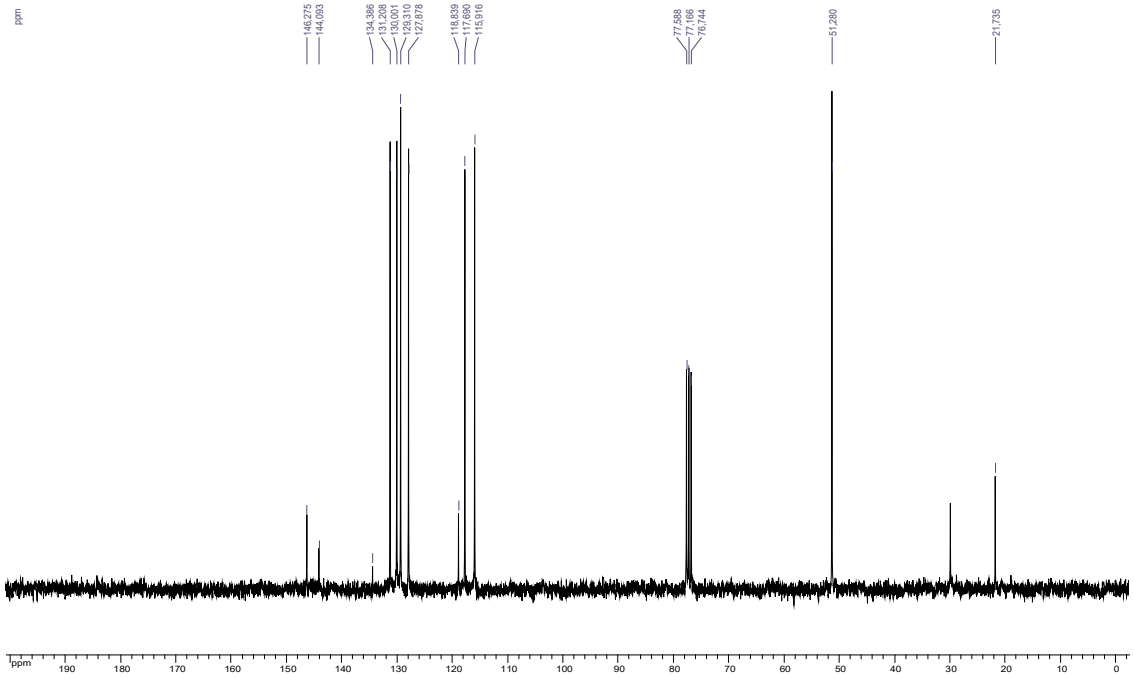

IV.7. Compound (*E*-2a).

^{1}H NMR ($CDCl_3$, 500 MHz)

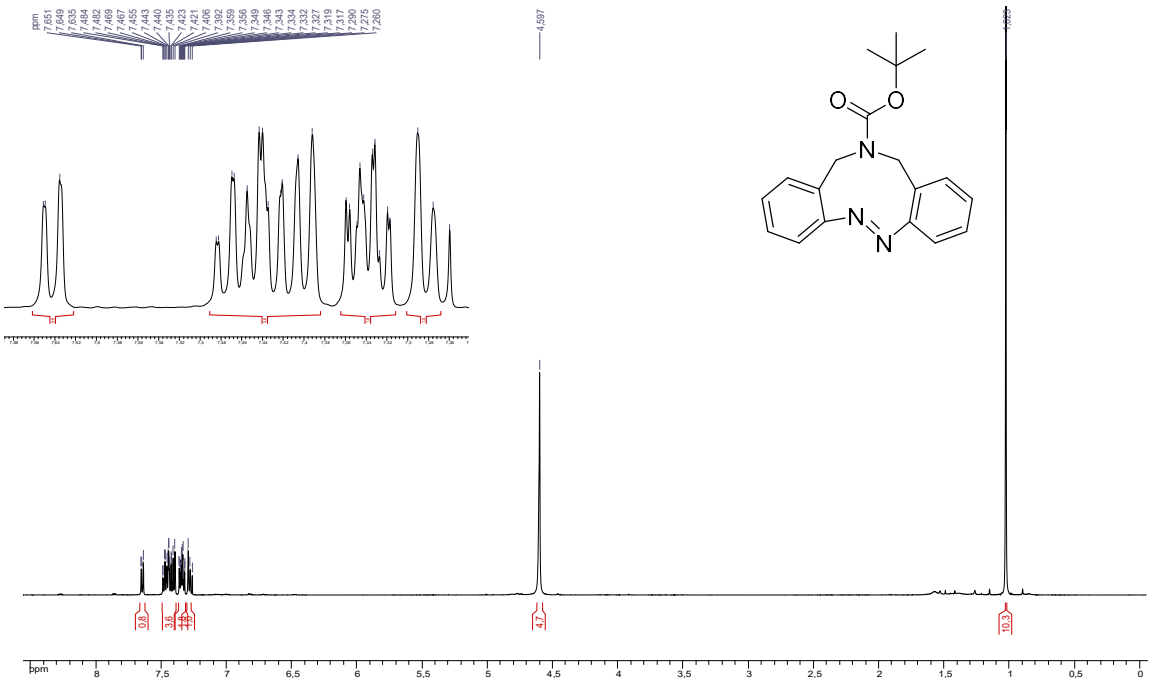

^{13}C NMR ($CDCl_3$, 75 MHz)

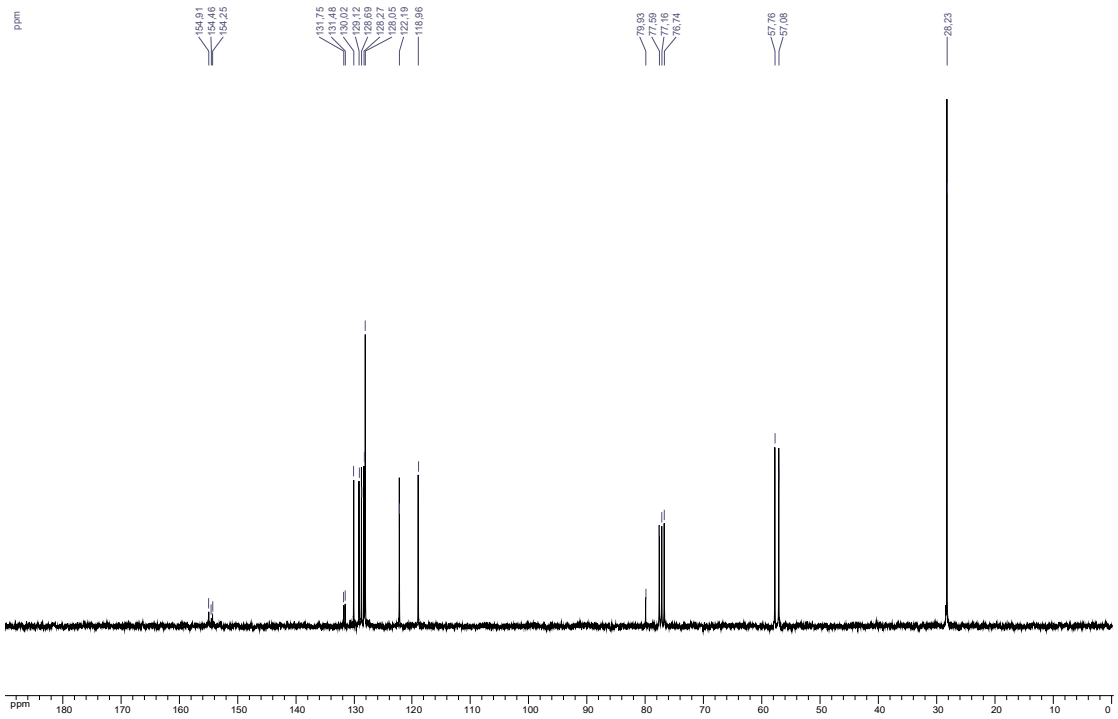

IV.8. Compound (*Z*-2a).

^{1}H NMR ($CDCl_3$, 500 MHz)

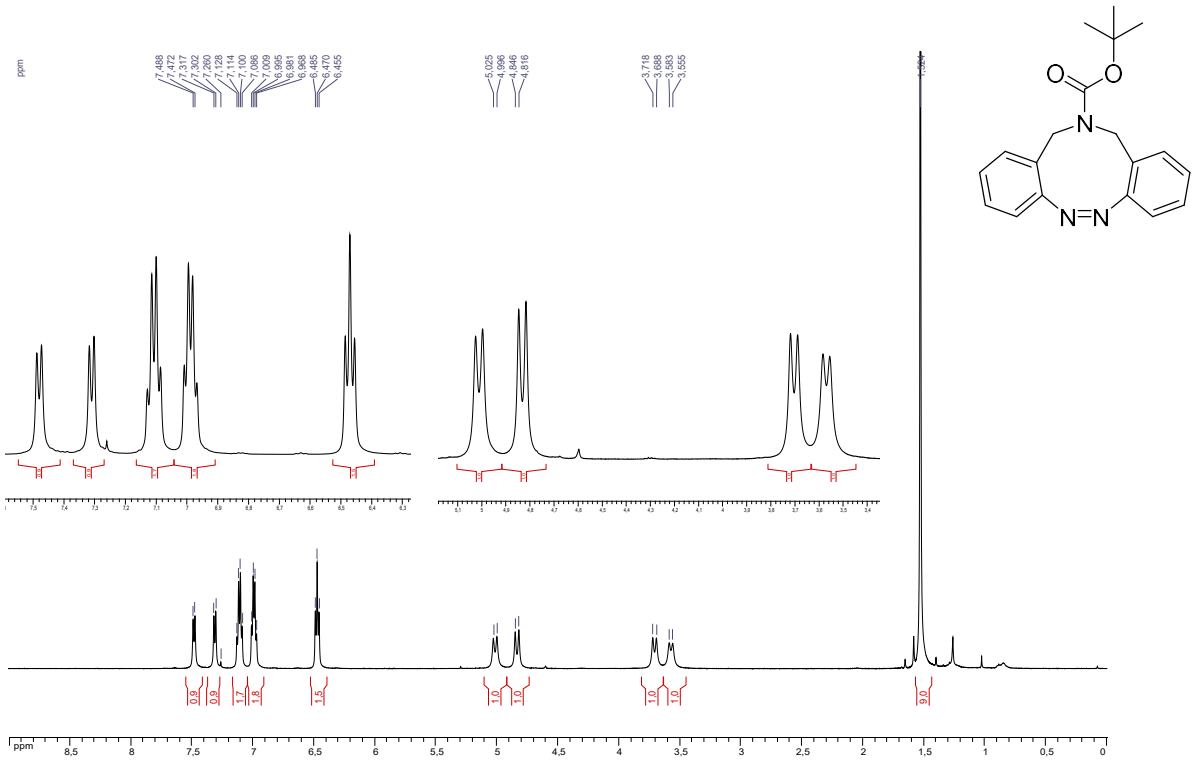

^{13}C NMR ($CDCl_3$, 75 MHz)

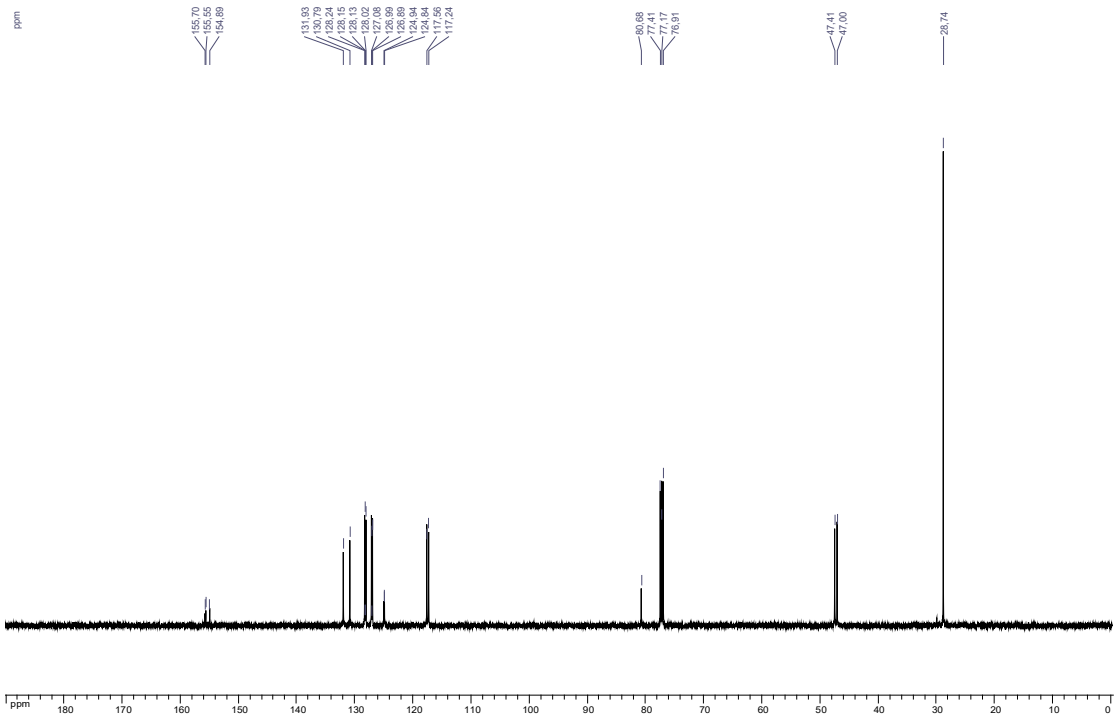

IV.9. Compound (*E*-2b).

^{1}H NMR ($CDCl_3$, 300 MHz)

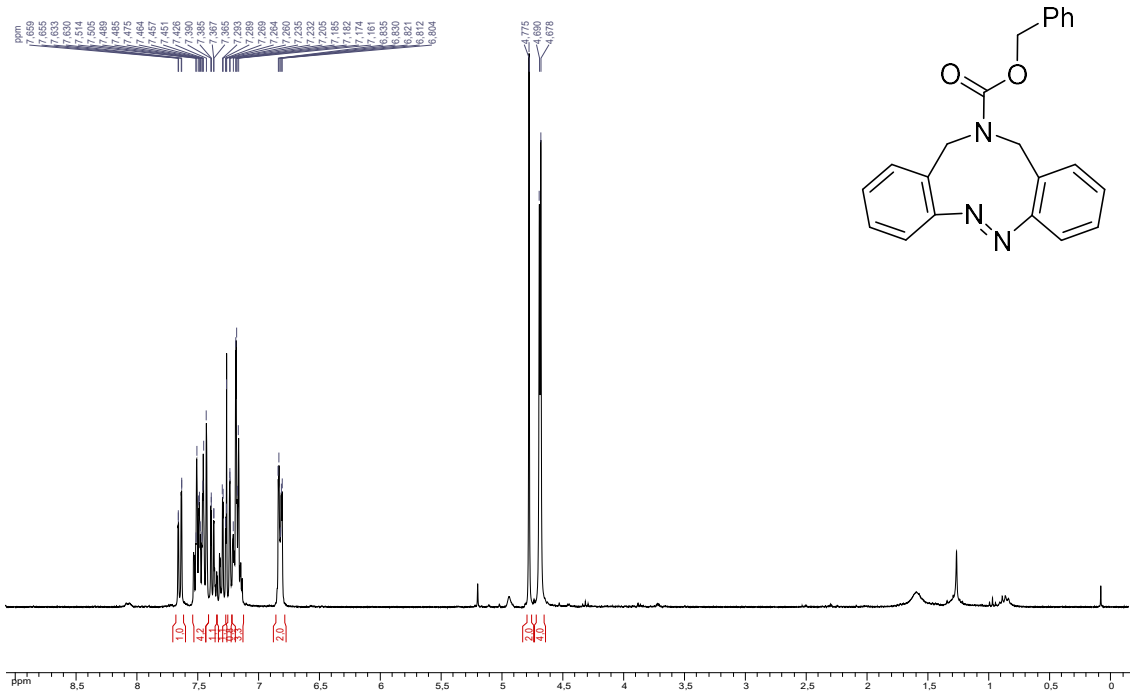

^{13}C NMR ($CDCl_3$, 75 MHz)

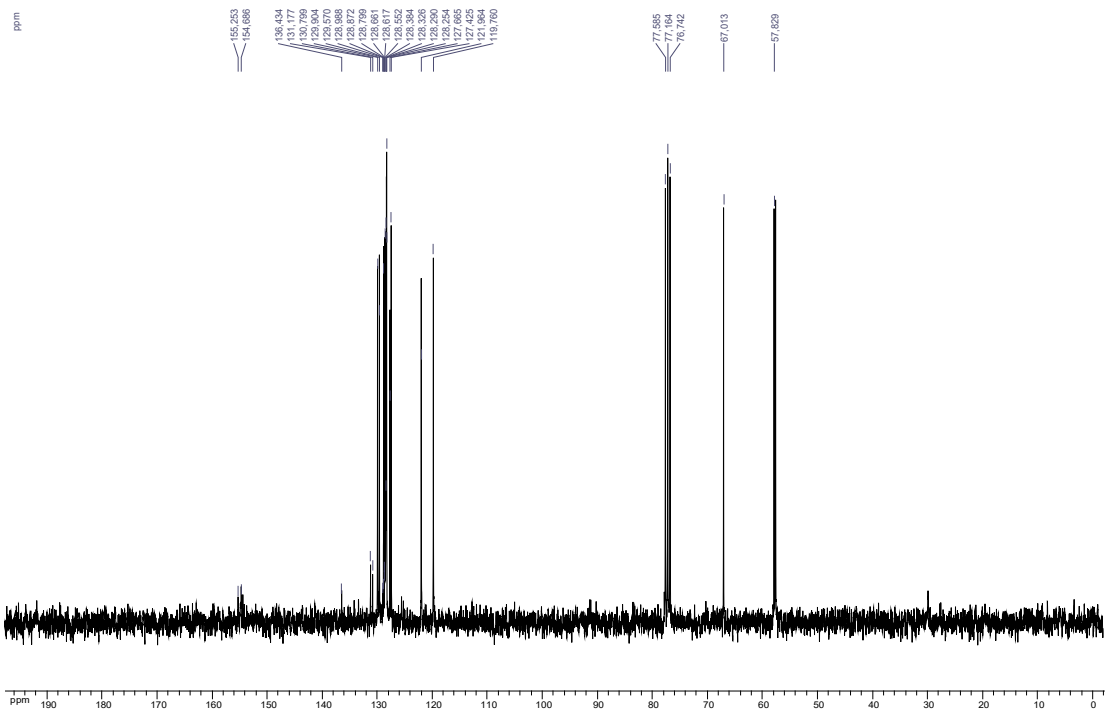

IV.10. Compound (*Z*-2b).

^{1}H NMR ($CDCl_3$, 300 MHz)

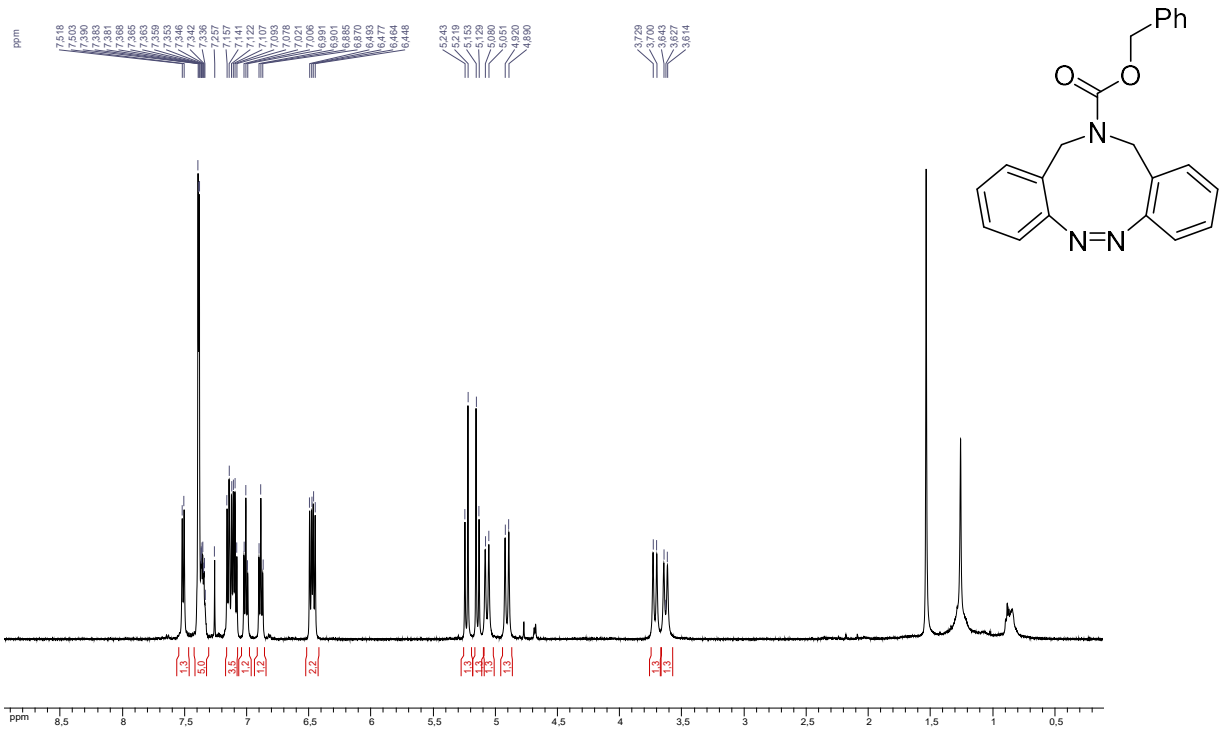

^{13}C NMR ($CDCl_3$, 75 MHz)

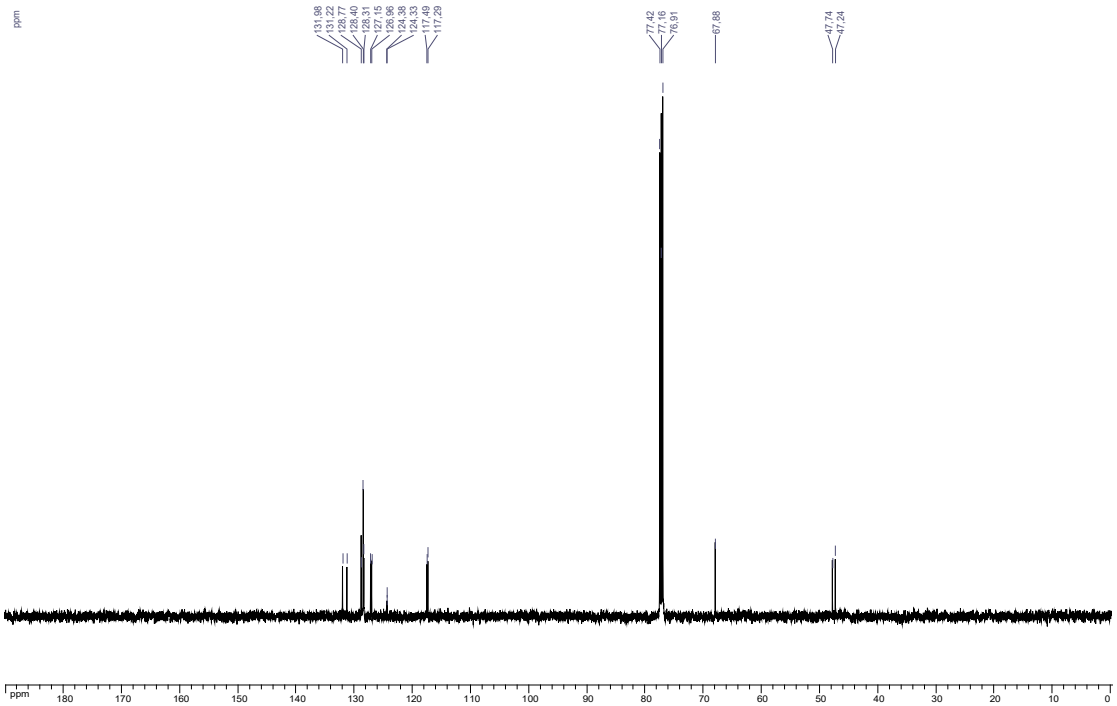

IV.11. Compound (*E*-2c).

^{1}H NMR ($CDCl_3$, 300 MHz)

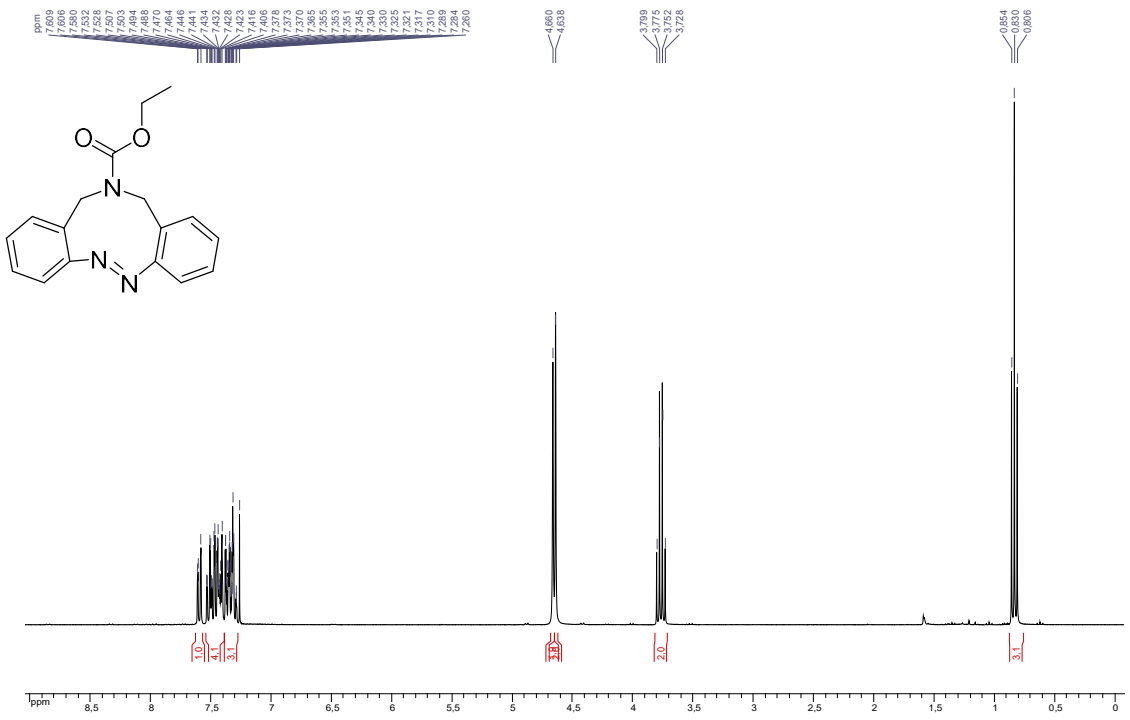

^{13}C NMR ($CDCl_3$, 75 MHz)

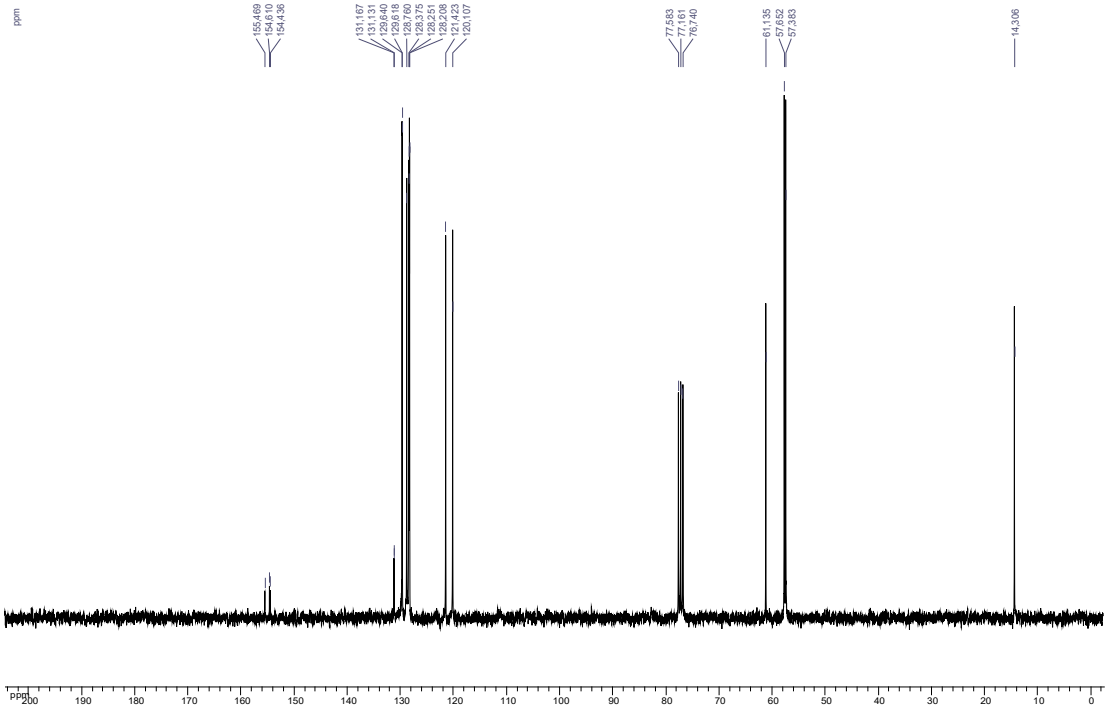

IV.12. Compound (*Z*-2c).

^{1}H NMR ($CDCl_3$, 300 MHz)

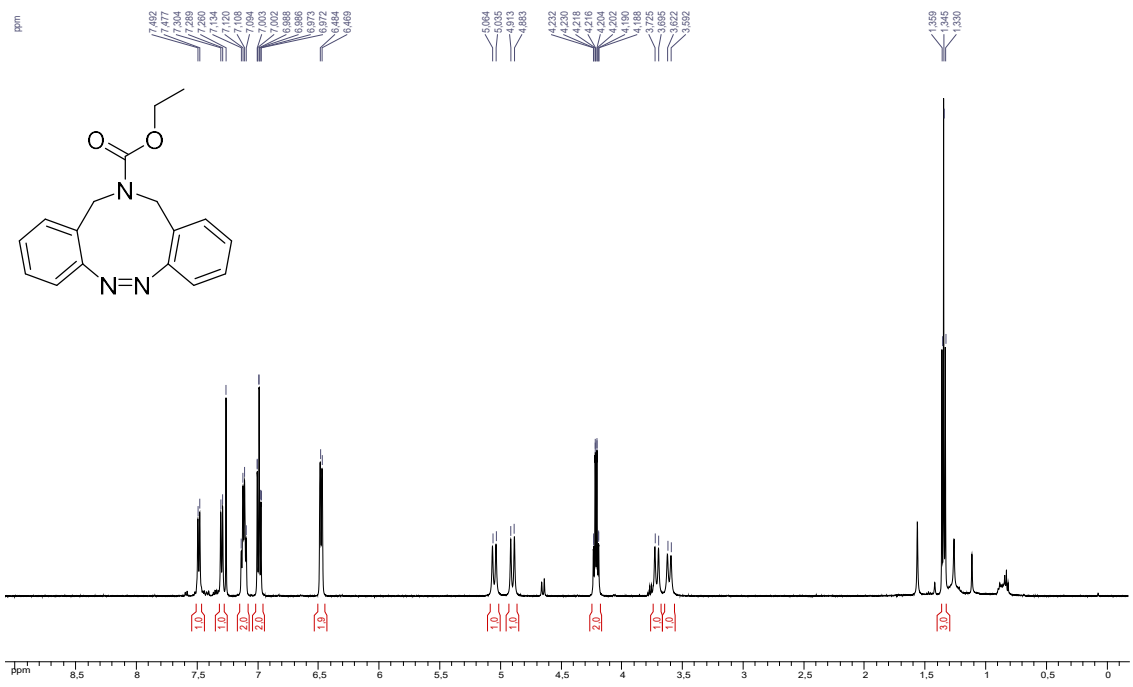

^{13}C NMR ($CDCl_3$, 75 MHz)

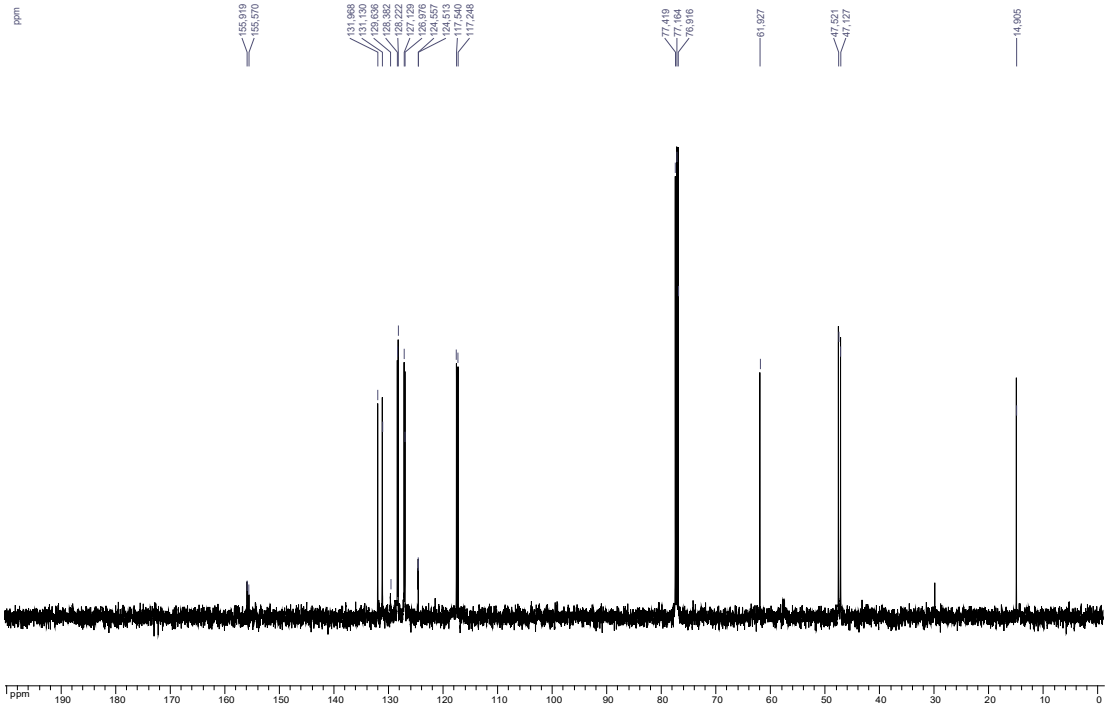

IV.13. Compound (*E*-4).

^{1}H NMR ($CDCl_3$, 300 MHz)

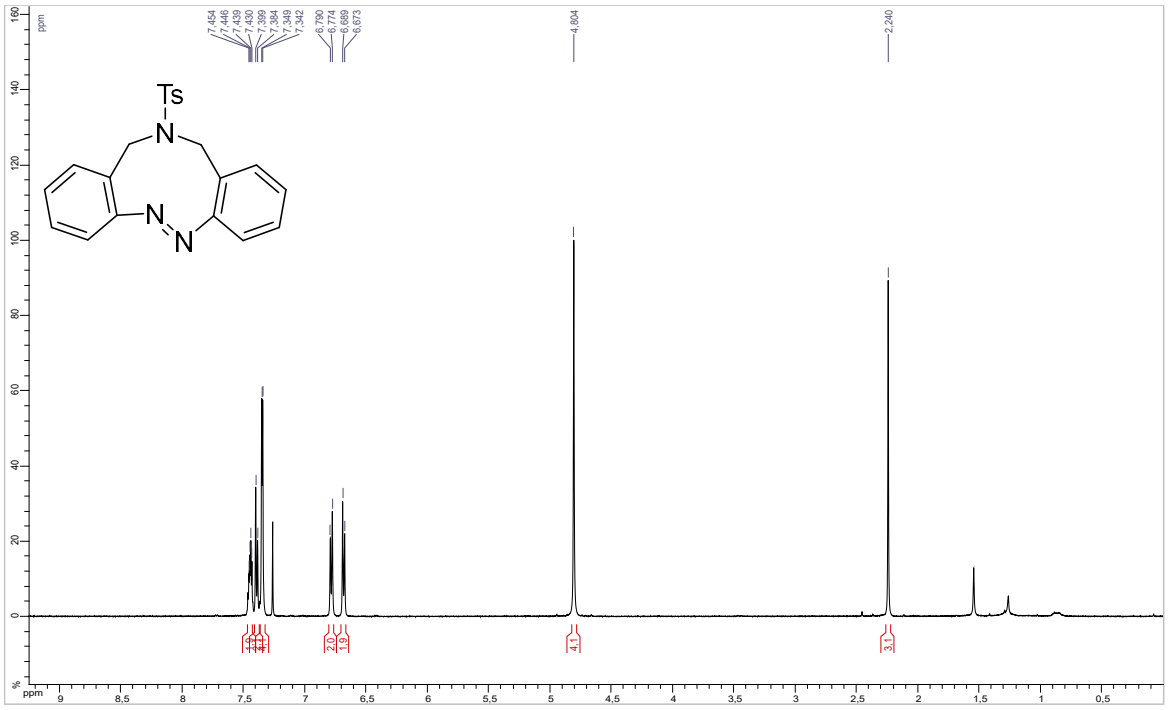

^{13}C NMR ($CDCl_3$, 75 MHz)

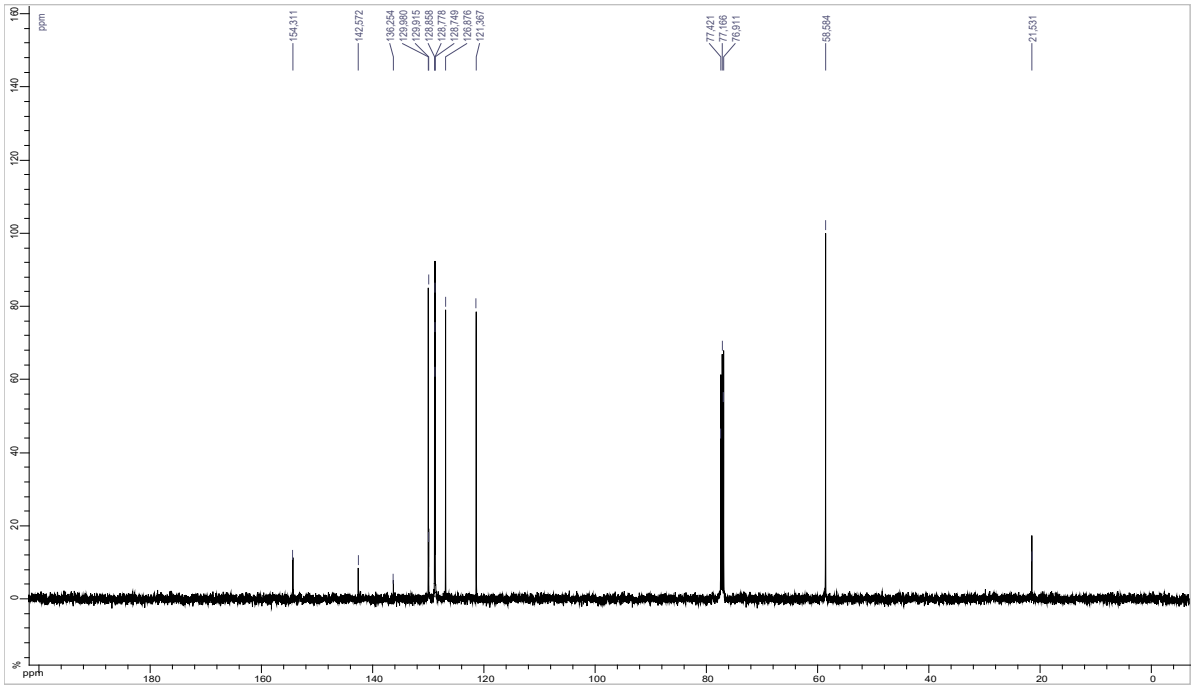

IV.14. Compound (*Z*-4).

^{1}H NMR ($CDCl_3$, 300 MHz)

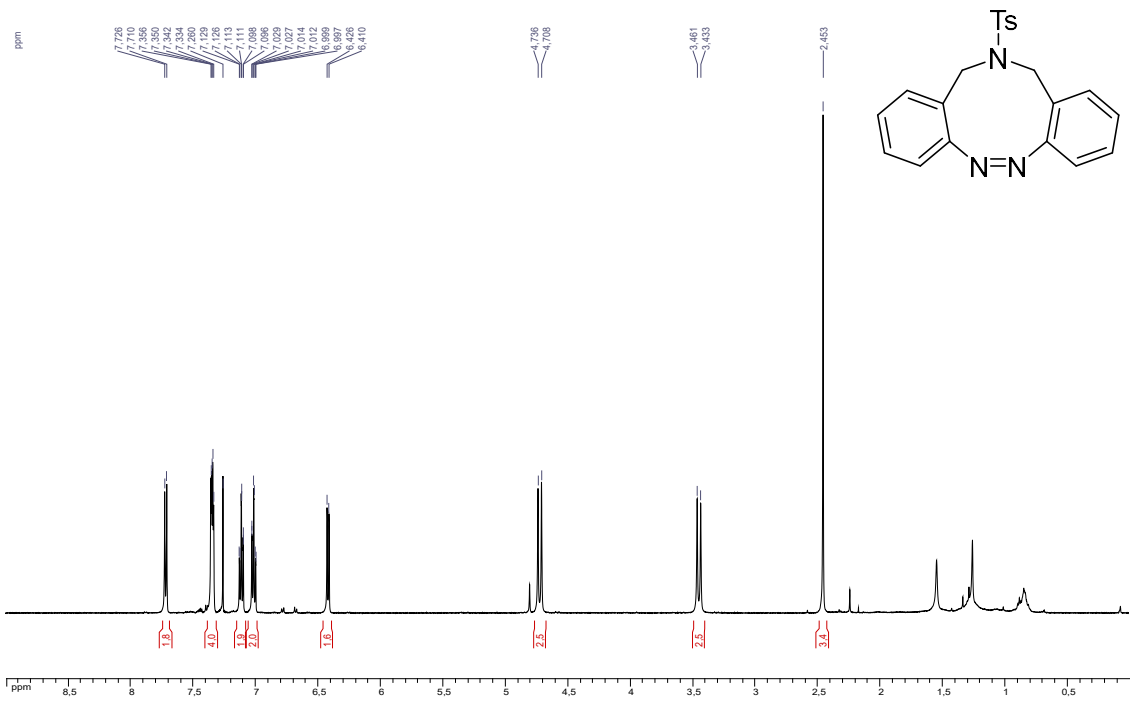

^{13}C NMR ($CDCl_3$, 75 MHz)

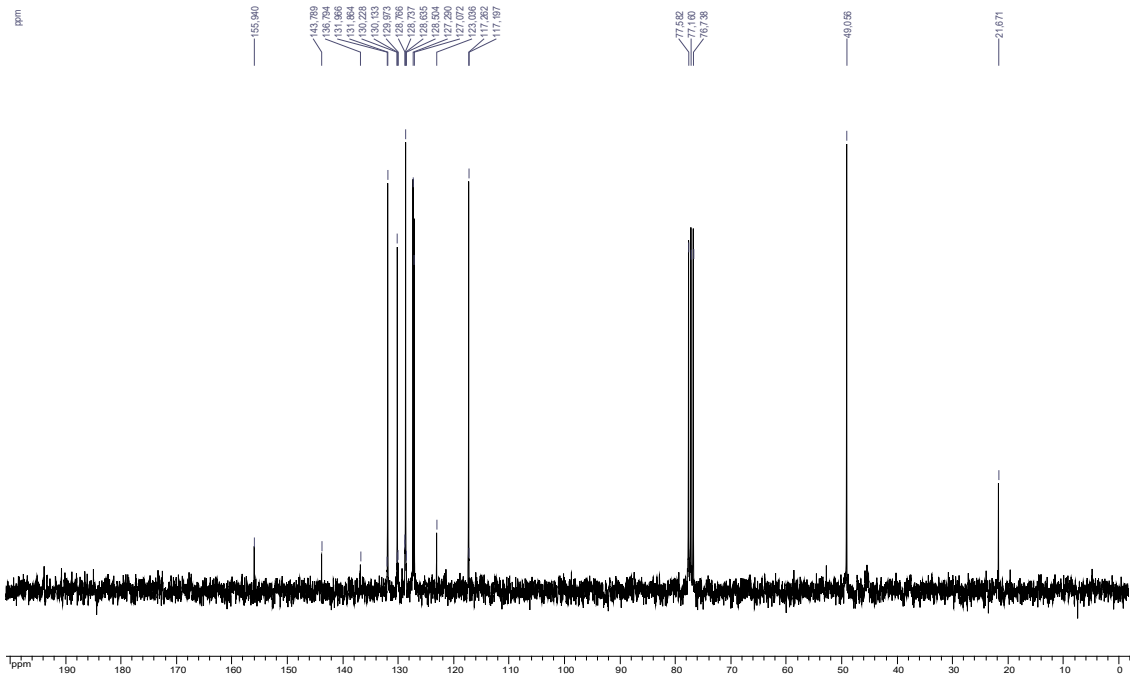

IV. X-Ray crystal structure determination.

Crystallographic data collection, structure determination and refinement.

The five following compounds (***Z-4***, ***Z-2a***, ***E-2a***, ***E-2c*** and ***Z-2c***) were crystallized in a manner suitable to Single Crystal X-ray Diffraction analyses that were all performed using a RIGAKU XtaLabPro diffractometer equipped with a Mo microfocus sealed tube generator coupled to a double-bounce confocal Max-Flux® multilayer optic and a HPAD PILATUS3 R 200K detector. Data collection was carried out using the software *CrysAlisPro 1.171.39.46*[1] at room temperature for ***Z-4***, ***E-2c*** and ***Z-2c*** but at low temperature for ***Z-2a,*** and ***E-2a***, 100 and 173 K respectively. SCALE3 ABSPACK scaling algorithm implemented within *CrysAlisPro* was applied to the processed data for the empirical absorption correction using spherical harmonics. The five structures were readily solved by intrinsic phasing methods (*SHELXT* program)[2] and refined by full-matrix least-squares methods on F^2 using *SHELX-L*.[3] All non-hydrogen atoms of the molecules of interest improved by anisotropic refinement. Most of the H atoms were identified in difference maps. Methyl H atoms were idealized and included as rigid groups allowed to rotate but not tip and refined with U_{iso} set to $1.5U_{eq}$(C) of the parent carbon atom. All other H atoms bound to carbon atoms were positioned geometrically and refined with U_{iso} set to $1.2U_{eq}$(C) of the parent carbon atom.

The five compounds are built around a nine-membered triazine ring with a pseudo molecular point group Cs, the bisectional mirror σ_d passing through the double bond between two nitrogen atoms and the facing third one separated from them by three carbon atoms on each side. ***Z-4***, ***Z-2a***, and ***Z-2c*** adopt a *Z*-conformation related to the N=N bond. These 9-membered heterocycles exhibit an evident chair-boat conformation[4] with the single N1 as the back of the chair. Contrasting with the Cs symmetric molecule ***Z-4***, the acetate substituents to N1 in ***Z-2a*** and ***Z-2c*** break that symmetry by lying either on both sides of the σ_d pseudo-mirror. The dihedral angles between the phenyl rings flanking the folded heterocycle range between 58.6 and 64.7° for ***Z-4***, 65.1 and 67.7° for ***Z-2a***, and close to 72° for ***Z-2c***. With respect to ***E-2a*** and ***E-2c***, this is the conformer E of the respective latter compounds which is found. In ***E-2a*** the double bond appears to a certain extent short (< 1Å) and almost coplanar to the ring made of carbon atoms implying a static disorder of the overall structure which has been refined over two sites slightly shifted to each other by *ca* 0.3Å and with refined occupancy ratio of 0.79(1):0.21(1). This permitted the restitution of the correct geometry around the N=N double azo bond with lengths of N2(*B*)=N3(*B*) =1.254(2) (*1.243(10)*)Å close to than observed at rt for ***E-2c***, 1.245(2) Å and in similar compounds[5] including the Z conformers from this work. Among these five presented structures, ***E-2a*** is not the unique example having two conformers in the asymmetric unit (***au***) of the obtained crystals: indeed, ***Z-4*** and ***Z-2a*** crystallized in the triclinic space group, P -1, with two copies in equivalent ratio. If the overall rmsd between the two conformers of ***Z-4*** is low, *ca* 0.19Å, these are the two isomers (with respect of the relative acetate group orientation), which are present in the ***au*** displaying significant differences in the opening of the triazonine core. The nine-membered ring in the *E*-conformers displays an apparent 'twist-chair-chair' conformation at the expense in ***E-2a*** of some EADP restraints and RIGU restraints applied throughout the structure to model the anisotropic displacement parameters impacted by the molecular disorder. In other words, the conformer Z of the dibenzotriazonine group displays a U-shape (or folded butterfly) when the E one appears unfolded or more and less flat.

X-ray crystallography data collection parameters and structure refinement statistics are reported in table ***S1***. Ortep[6] views are shown in Figure ***S1***. CCDC 1961684, 2007074-2007075, and 2056225-2056226 (compounds ***Z-4***, ***Z-2a***, ***E-2a***, ***E-2c*** and ***Z-2c*** respectively) contain the supplementary crystallographic data for this paper. These data can be obtained free of charge from The Cambridge Crystallographic Data Centre via www.ccdc.cam.ac.uk/data_request/cif.

[1] O.D. Rigaku (2015). *CrysAlis PRO*. Rigaku Oxford Diffraction, Yarnton, Oxfordshire, England.
[2] G. M. Sheldrick, *Acta Crystallogr.* 2015, **A71**, 3-8.
[3] G. M. Sheldrick, *Acta Crystallogr.* 2015, **C71**, 3-8.
[4] D.G. Evans, J. C. A. Boeyens, *Acta Crystallogr*. 1990, **B46**, 524-532.
[5] (*a*) C. He, H. Gao, G. H. Imler, D. A. Parrish, J. M. Shreeve, *J. Mater. Chem. A*, 2018, **6**, 9391–9396; (*b*) J. Zhang, J. M. Shreeve, *J. Phys. Chem. C*, 2015, **119**, 12887–12895.
[6] (*a*) M. N. Burnett, C. K. Johnson, 1996, *ORTEPIII*. Report ORNL-6895. Oak Ridge National Laboratory, Tennessee, USA; (*b*) C. F. Macrae, P. R. Edgington, P. McCabe, E. Pidcock, G. P. Shields, R. Taylor, M. Towler, J. van de Streek, *J. Appl. Cryst.* 2006, **39**, 453-457.

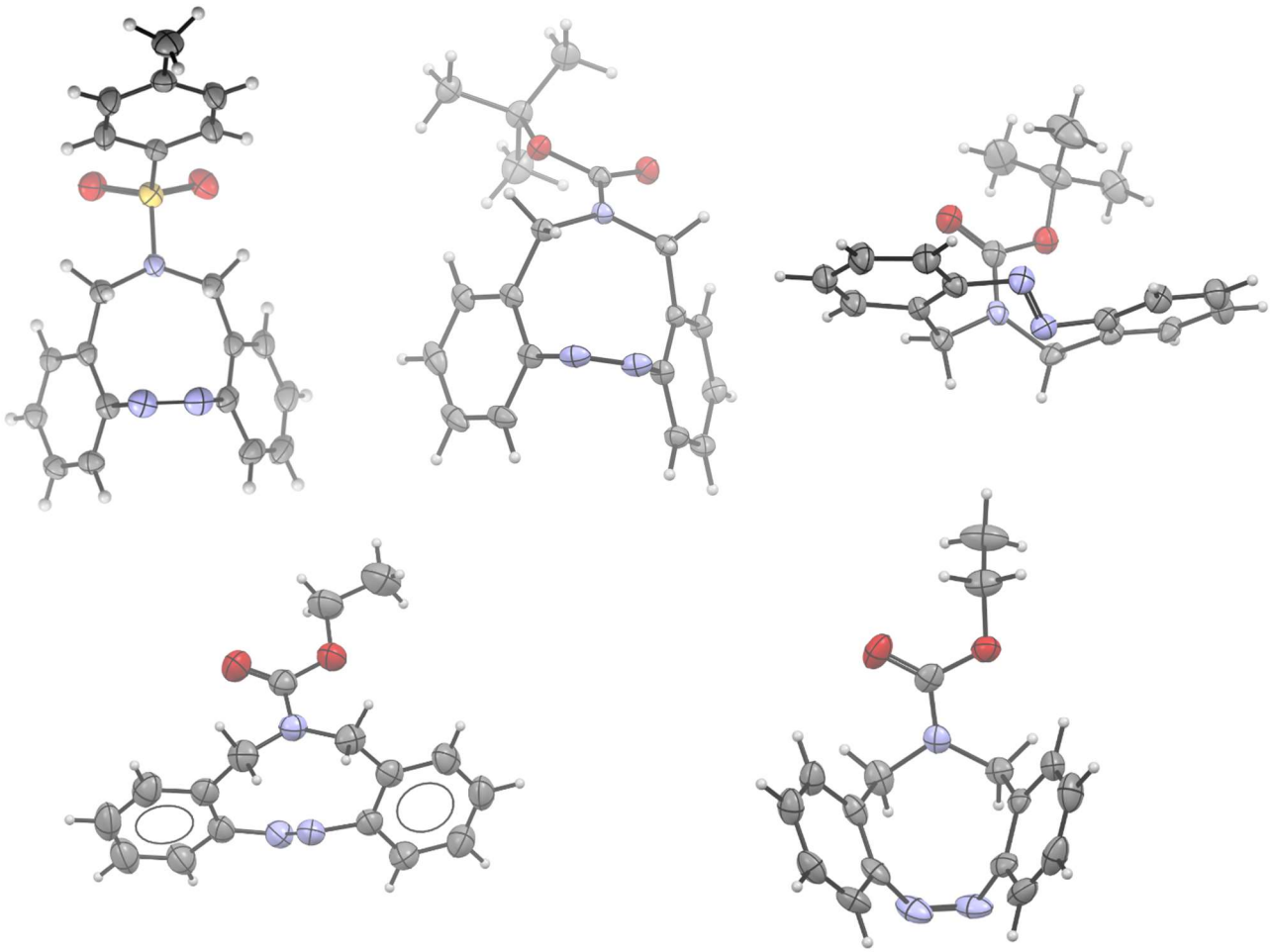

Figure S1. *Ortep plot of one conformer (out of two present in the asu) of* ***Z-4*** *(upper left), idem for* ***Z-2a*** *(upper middle), and of* ***E-2a*** *(major site, upper right). Ortep views for* ***E-2c*** *and* ***Z-2c*** *are shown respectively at lower left and right position of the frame. Ellipsoids are drawn at 50% of probability and hydrogen atoms, with sphere radius of arbitrary size.*

Overlay of *Z*-isomers of **2a** (in pale green), **2c** (in grey) and **4** (in pink):

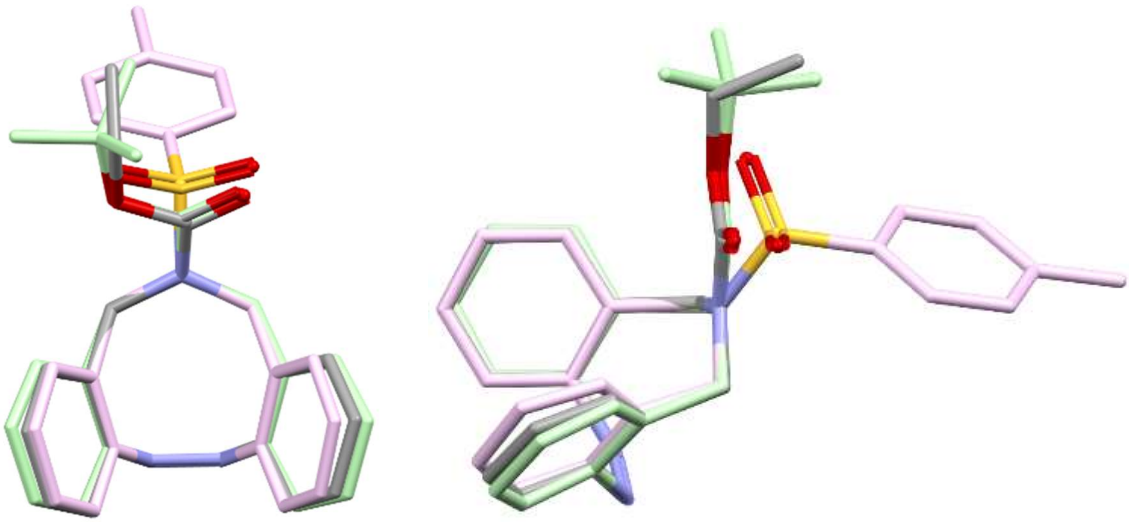

Table S1. *Crystal data and structure refinement for* ***Z-4****,* ***Z-2a****,* ***E-2a****,* ***E-2c*** *and* ***Z-2c****.*

Identification code		***Z*-4**	***Z*-2a**	***E*-2a**	***E*-2c**	***Z*-2c**
CRYSTAL DATA						
Name		(*Z*)-12-Tosyl-12,13-dihydro-11*H*-dibenzo[*c*,*h*][1,2,6]triazonine	*tert*-Butyl (*Z*)-11,13-dihydro-12*H*-dibenzo[*c*,*h*][1,2,6]triazonine-12-carboxylate	*tert*-Butyl (*E*)-11,13-dihydro-12*H*-dibenzo[*c*,*h*][1,2,6]triazonine-12-carboxylate	Ethyl (*E*)-11,13-dihydro-12*H*-dibenzo[*c*,*h*][1,2,6]triazonine-12-carboxylate	Ethyl (*Z*)-11,13-dihydro-12*H*-dibenzo[*c*,*h*][1,2,6]triazonine-12-carboxylate
Structure		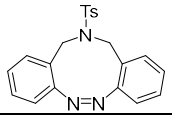	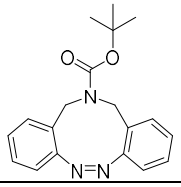	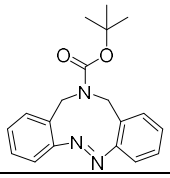	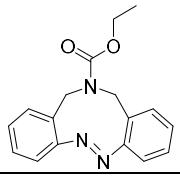	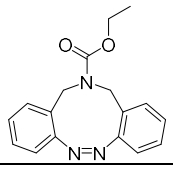
Empirical formula		$C_{21}H_{19}N_3O_2S$	$C_{19}H_{21}N_3O_2$	$C_{19}H_{21}N_3O_2$	$C_{17}H_{17}N_3O_2$	$C_{17}H_{17}N_3O_2$
Formula weight		377.45	323.39	323.39	295.33	295.33
Crystal system, Space group		Triclinic, P -1	Triclinic, P -1	Monoclinic, P 2_1/c	Orthorhombic, P $2_12_12_1$	Orthorhombic, P bca
Unit cell dimensions (Å,°)	a | Å	12.1589(9)	9.4527(2)	13.7733(4)	5.0393(3)	12.2994(4)
	b	12.2886(9)	11.1113(3)	10.3424(3)	11.5613(6)	9.1580(9)
	c	13.5265(10)	17.2833(5)	12.3133(4)	26.3881(15)	26.4451(10)
	α °	81.017(7)	72.180(2)	90	90	90
	β °	89.628(8)	86.927(2)	91.874(3)	90	90
		71.449(6)	81.304(2)	90	90	90
Volume (Å^3)		1123.07(18)	1708.28(8)	1753.08(10)	1537.41(16)	2978.73(19)
Z, Calculated density (Mg/m^3)		4, 1.326	4, 1.257	4, 1.225	4, 1.276	8, 1.317
Absorption coefficient (mm^{-1})		0.192	0.083	0.081	0.086	0.089
F(000)		792	688	688	624	1248
Crystal size (mm)		0.55 x 0.45 x 0.28	0.28 x 0.22 x 0.03	0.50 x 0.45 x 0.30	0.32 x 0.07 x 0.04	0.40 x 0.30 x 0.20
DATA COLLECTION						
Diffractometer		Rigaku XtaLabPro mm003 diffractometer with Pilatus 200K Hybrid pixel array detector (HPAD)				
Wavelength (Å)		0.71073				
Temperature (K)		293(2)	100(2)	173(2)	293(2)	173(2)
θ range for data collection (°)		3.771 to 27.455	3.562 to 27.482	3.671 to 27.100	3.524 to 26.369	2.878 to 26.367
Limiting indices		-15 ≤ h ≤ 15, -15 ≤ k ≤ 15, -17 ≤ l ≤ 17	-12 ≤ h ≤ 12, -14 ≤ k ≤ 14, -22 ≤ l ≤ 22	-17 ≤ h ≤ 17, -12 ≤ k ≤ 13, -15 ≤ l ≤ 15	-6 ≤ h ≤ 6, -12 ≤ k ≤ 14, -31 ≤ l ≤ 32	-15 ≤ h ≤ 15, -10 ≤ k ≤ 11, -32 ≤ l ≤ 33
Reflections collected unique R(int)		52160 / 8484 0.0419	27891 / 7635 0.0452	19111 / 3825 0.0644	9387 / 3072 0.0379	20431 / 3045 0.0223
Completeness to θ_{full} (%)		99.2	99.4	99.6	99.1	99.9
Absorption correction		Semi-empirical from equivalents				
Max. and min. transmission		1.000 and 0.748	1.000 and 0.787	1.000 and 0.382	1.000 and 0.439	1.000 and 0.894
REFINEMENT						
Refinement method		Full-matrix least-squares on F^2				

Data / restraints / parameters	8476 / 0 / 489	7611 / 0 / 439	3825 / 441 / 404	3063 / 0 / 202	3045 / 0 / 201
Goodness-of-fit on F^2	1.063	1.047	1.069	1.058	1.022
Final R indices [$I>2\sigma(I)$]	0.0408, 0.1179	0.0448, 0.1149	0.0534, 0.1396	0.0384, 0.0931	0.0397, 0.1035
R indices (all data)	0.0459, 0.1217	0.0569, 0.1217	0.0591, 0.1454	0.0498, 0.0985	0.0435, 0.1060
Absolute structure parameter	-	-	-	0.4(17)	-
Extinction coefficient	-	-	-	0..025(5)	0.0024(7)
Largest diff. peak and hole (e. Å^3)	0.228 and -0.430	0.315 and -0.264	0.338 and -0.330	0.186 and -0.213	0.207 and -0.145

V. Photophysical properties of 2a-c and 4.

Absorption spectra and irradiation experiments were performed in spectroscopic grade acetonitrile (Carlo Erba). UV-vis absorption spectra were recorded on Cary 100 or Cary 5000 spectrophotometer from Agilent Technologies. Photoisomerization reactions were induced by a Hg/Xe Lamp Hamamatsu LC8 Lightningcure, whose spectral line was selected by means of an interference filter (Semrock FF01-315/15-25 + FF01-320/40-25, FF01-335/7-25, FF01-370/10-25, FF01-438/24-25). The incident lamp power was measured with an Ophir PD300-UV photodiode. Photoisomerization quantum yields and fatigue resistances were determined using a home-made setup, which allows to collect absorption spectra with high rates, under continuous irradiation. A Xenon lamp (75 W) was used as a probing light source, and a Hg/Xe lamp, placed at 90° with respect to the incident beam, was used to induce the photochromic reaction in the sample, placed in a cuvette and thoroughly stirred. Spectra were recorded every 0.2 s, with a spectrometer coupled with a CCD camera (Roper Scientific and Princeton Instruments, respectively). The quantum yield values were then extracted by fitting the time-dependent absorbance evolution according to the photokinetic equation of a photochrome, using an algorithm implemented in Igor (Wavemetrics) software. Since the thermal back reaction was found to be very slow in all solvents at room temperature, it was considered negligible in the time-scale of the photokinetic measurements. The overall differential photokinetic equation related to the *E*-*Z* light-induced interconversion[7] can be written:

$$\frac{dC_Z}{dt} = -\frac{dC_E}{dt} = \Phi_{EZ} \times I_E^{abs}(\lambda_{irr}, t) - \Phi_{ZE} \times I_Z^{abs}(\lambda_{irr}, t) \qquad \text{(Eq. 1)}$$

where Φ_{EZ} is the quantum yield for the $E \rightarrow Z$ isomerization, Φ_{ZE} is the quantum yield for the $Z \rightarrow E$ isomerization and I^{abs} is the time-dependent intensity absorbed by the compound at the irradiation wavelength λ_{irr}:

$$I_E^{abs}(\lambda_{irr}, t) = \left[\frac{1-10^{-Abs(\lambda_{irr},t)}}{Abs(\lambda_{irr},t)}\right] \times I_0(\lambda_{irr})\varepsilon_E(\lambda_{irr})\ell C_E(t) \qquad \text{(Eq. 2)}$$

$$I_Z^{abs}(\lambda_{irr}, t) = \left[\frac{1-10^{-Abs(\lambda_{irr},t)}}{Abs(\lambda_{irr},t)}\right] \times I_0(\lambda_{irr})\varepsilon_Z(\lambda_{irr})\ell C_Z(t) \qquad \text{(Eq. 3)}$$

with Abs(λ_{irr},t) the absorbance value at the irradiation wavelength during the time of the experiment. A numerical iterative fitting algorithm based on Eq. 1-3 provides the values of Φ_{EZ} and Φ_{ZE}, in all solvents and at the different irradiation wavelengths investigated.

We calculated the conversion yields (α_Z) reached at the PSSs, *i.e.*, the relative ratio between the *E* and the *Z* isomer, from the absorption spectra of the irradiated mixtures, according to Eq. 1:

$$\alpha_Z = \frac{A_{PSS} - A_E}{A_Z - A_E} \qquad \text{Eq. 1}$$

[7] K. Nakatani, J. Piard, P. Yu, R. Métivier in Photochromic Materials: Preparation, Properties and Applications, 1st ed. (Eds.: H. Tian, J. Zhang), Wiley-VCH, Weinheim, 2016, pp. 1 – 45.

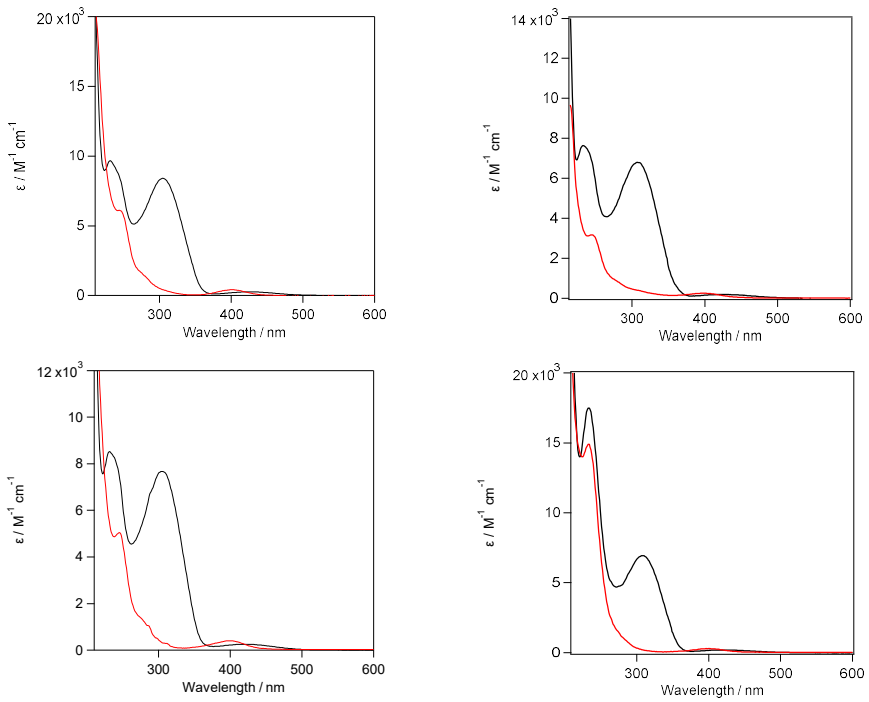

Compound	λ_{max} / nm	ε / M^{-1} cm^{-1}	Compound	λ_{max} / nm	ε / M^{-1} cm^{-1}
E-**2a**	426 (n-π*) 303 (π-π*) 231	260 8390 9680	*E*-**2c**	420 (n-π*) 304 (π-π*) 231	253 7674 8519
Z-**2a**	401 (n-π*) 244 (π-π*)	410 6100	*Z*-**2c**	400 (n-π*) 245 (π-π*)	403 5048
E-**2b**	423 (n-π*) 307 (π-π*) 232	190 6800 7640	*E*-**4**	422 (n-π*) 308 (π-π*) 233	190 6940 17550
Z-**2b**	400 (n-π*) 245 (π-π*)	250 3170	*Z*-**4**	399 (n-π*) 234 (π-π*)	280 14900

Figure S2. *Absorption spectra in CH_3CN of the E- (black) and the Z-isomers (red) of* ***2a*** *(top left),* ***2b*** *(top right),* ***2c*** *(bottom left) and* ***4*** *(bottom right).*

Compound **4** is not available in the pure *E*- nor in the pure *Z*-form. The spectra have been performed with *E*:*Z* mixtures of 70:30 or 7:93, verified by ^{1}H NMR. From the spectra of the two solutions, if the concentration is known, it is possible to extract the spectra of the two pure isomers, according to the following equations:

$$A_1 = \varepsilon^E c_1^E + \varepsilon^Z c_1^Z \qquad \text{and} \qquad A_2 = \varepsilon^E c_2^E + \varepsilon^Z c_2^Z$$

Where

$$c^E = c^0 \chi^E \qquad \text{and} \qquad c^Z = c^0 \chi^Z$$

By rearrangement

$$\varepsilon^Z = \frac{A_2 - \frac{A_1 c_2^E}{c_1^E}}{c_2^Z - \frac{c_1^Z c_2^E}{c_1^E}} \qquad \text{and} \qquad \varepsilon^E = \frac{A_1 - \varepsilon^Z c_1^Z}{c_1^E}$$

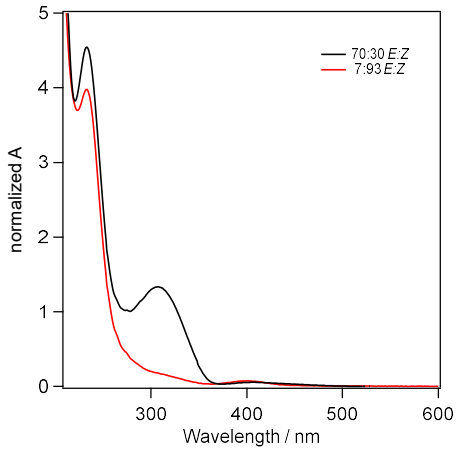

***Figure S3**. normalized absorbance spectra of the two mixtures E:Z 70:30 (black) and 7:93 (red) of **4** in CH_3CN.*

VI. Photoisomerization properties of 2a.

The Mauser plot[8] obtained from the irradiation at 334 nm (figure S4) shows a linear dependence of the absorbance values, meaning that no more than one process, *i.e.*, the photoisomerization, take place upon irradiation.

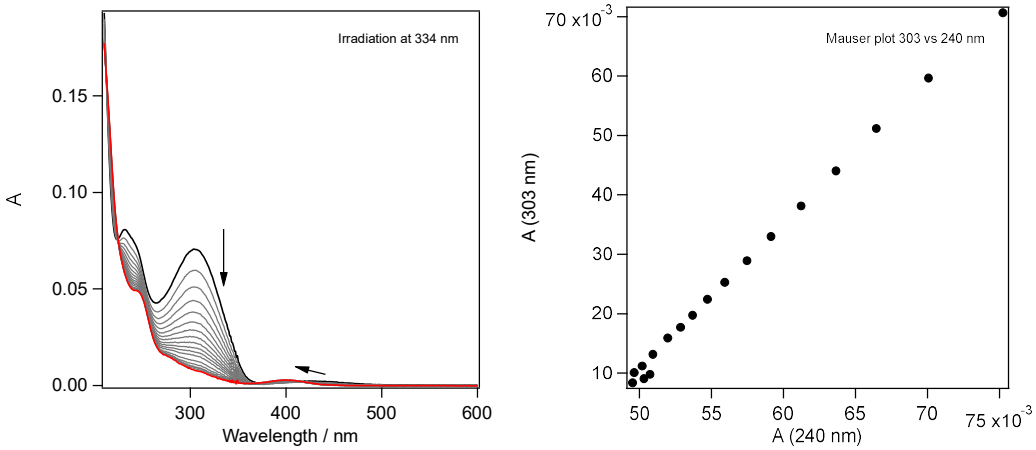

***Figure S4**. Left: absorbance variations of **2a** in CH_3CN upon irradiation at 334 nm; right: Mauser plot (303 nm vs 240 nm) related to the irradiation at 334 nm.*

[8](*a*) H. Mauser, Z. Naturfosch, 1968, **23b**, 1025; (*b*) H. Mauser, Formale Kinetik, Bertelsmann Universitatverlag, Dusseldorf, 1974.

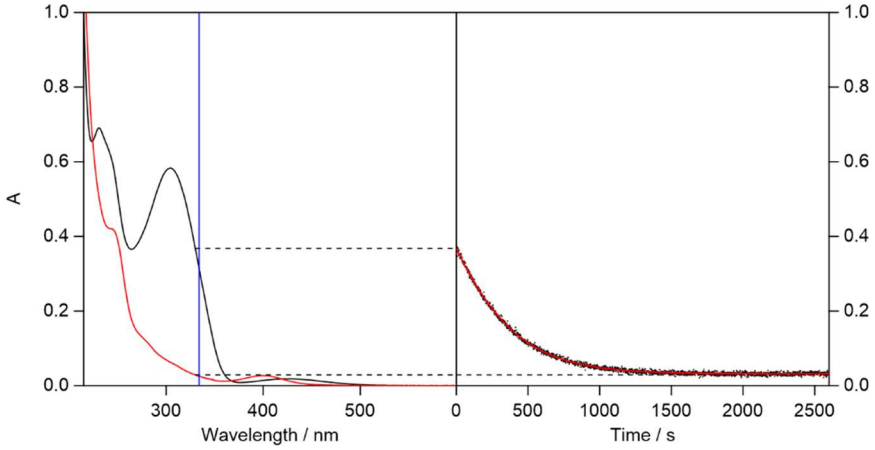

***Figure S5**. Left: absorption spectra of a solution 7.0 × 10^{-5} M of **2a** in CH_3CN before (black) and after (red) irradiation at 334 nm (blue bar); right: photokinetic profile at 330 nm and fitting (red line).*

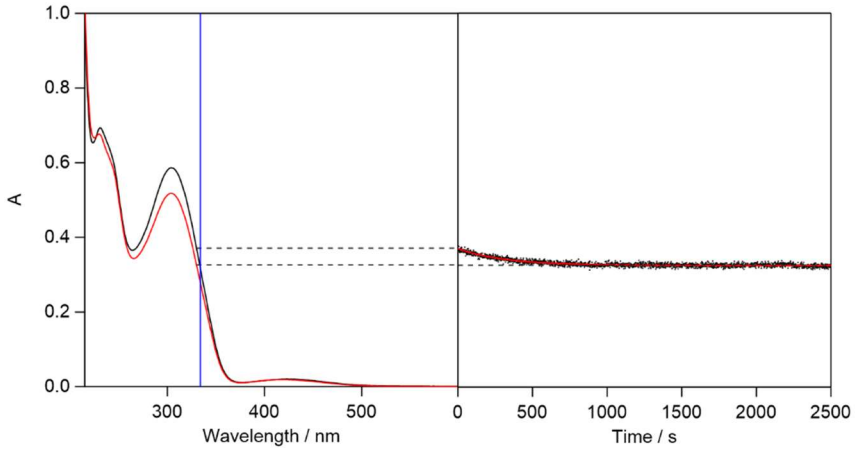

***Figure S6**. Left: absorption spectra of a solution 7.0 × 10^{-5} M of **2a** in CH_3CN before (black) and after (red) irradiation at 405 nm (blue bar); right: photokinetic profile at 330 nm and fitting (red line).*

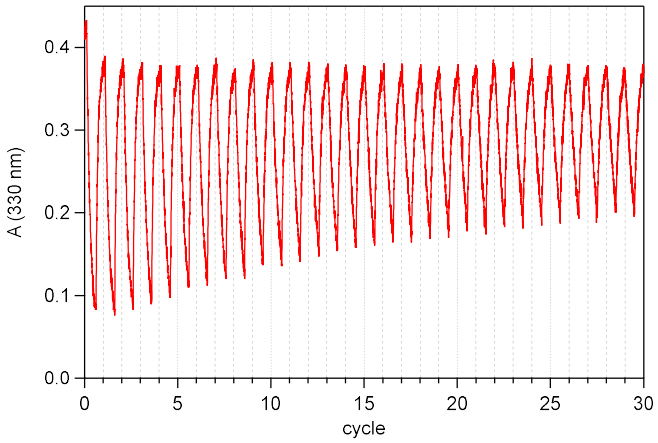

***Figure S7**. Fatigue resistance of a solution 8.1 × 10^{-5} M of **2a** in CH_3CN upon consecutive irradiations at 334 nm and 405 nm.*

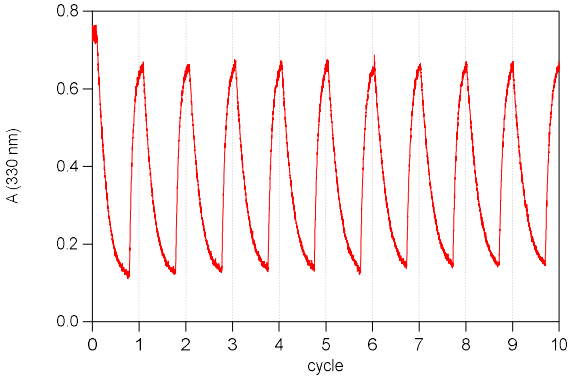

Figure S8. *Fatigue resistance of a solution 1.5 × 10^{-4} M of* ***2b*** *in CH_3CN upon consecutive irradiations at 334 nm and 405 nm.*

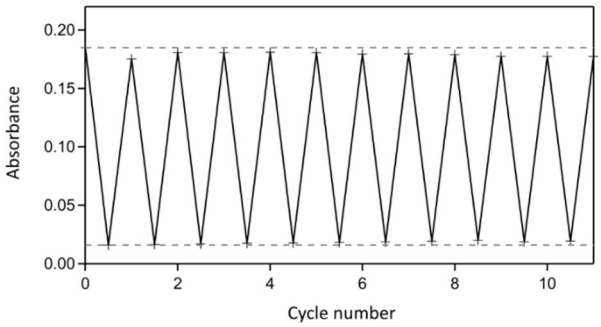

Figure S9. *Fatigue resistance of a solution 0.015 M of* ***4*** *in CH_3CN upon consecutive irradiations at 313 nm and 405 nm.*

λ_{irr} / nm	α_Z	Φ_{EZ}	σ	n	Φ_{ZE}	σ	n
313	0.90	0.15	0.04	3	0.33	0.08	3
334	0.93	0.13	0.02	4	0.50	0.1	4
365	0.42	0.122	0.009	3	0.44	0.08	3
405	0.14	0.08	0.03	3	0.33	0.03	3
436	0.45	0.15	0.02	4	0.50	0.1	4

Table S2. *Absorbance ratios, photoconversions and quantum yields with standard deviation (σ) and number of measurements (n) of* ***2a*** *in CH_3CN for all the irradiation wavelengths.*

λ_{irr} / nm	α_Z	Φ_{EZ}	σ	n	Φ_{ZE}	σ	n
334	0.96	0.121	0.007	3	0.30	0.04	3
405	0.10	0.14	0.03	4	0.56	0.04	4

Table S3. *Absorbance ratios, photoconversions and quantum yields with standard deviation (σ) and number of measurements (n) of* ***2b*** *in CH_3CN for all the irradiation wavelengths.*

λ_{irr} / nm	α_Z	Φ_{EZ}	σ	n	Φ_{ZE}	σ	n
334	0.97	0.197	0.003	3	0.23	0.08	3
405	0.18	0.14	0.02	3	0.390	0.007	3

Table S4. *Absorbance ratios, photoconversions and quantum yields with standard deviation (σ) and number of measurements (n) of* ***2c*** *in CH_3CN for all the irradiation wavelengths.*

λ_{irr} / nm	α_Z	Φ_{EZ}	σ	n	Φ_{ZE}	σ	n
334	0.98	0.17	0.01	3	0.2	0.2	3
405	0.30	0.21	0.03	3	0.35	0.02	3

Table S5. *Absorbance ratios, photoconversions and quantum yields with standard deviation (σ) and number of measurements (n) of* ***4*** *in CH_3CN for all the irradiation wavelengths.*

VII. Thermal isomerization and kinetic studies.

VII.1. Absorption evolution of *Z*-**2a** in the dark at 25°C.

Figure S10 shows the absorption of a solution of pure *Z*-isomer left in the dark at 25°C for 20 hours. Minor absorbance changes are ascribable to partial evaporation of the solvent.

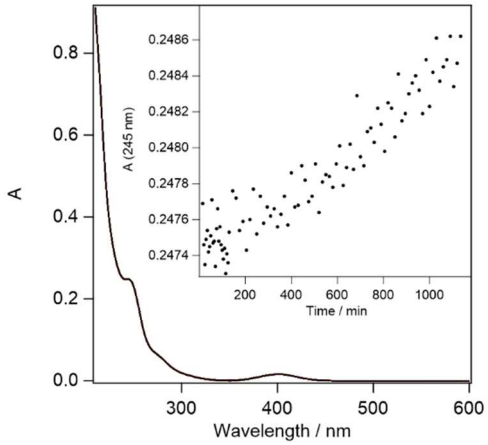

***Figure S10**. Absorption evolution of a CH_3CN solution of Z-**2a** in the dark at 25°C. The inset shows the absorbance variations at 245 nm over time.*

VII.2. Thermal isomerization of *Z*-**2a** and *E*-**2a** followed by ^{1}H NMR.

Thermal isomerization of *Z*-**2a** and *E*-**2a** was investigated by ^{1}H NMR experiments (Figures S11-18). The ratio between *E*- and *Z*-isomers was determined with the integration of the benzylic CH_2 protons of each isomer. If a singlet [δ 4.60 ppm] appears for these four protons in *E*-**2a**, four separate doublets [δ 5.01, 4.84, 3.71, 3.57 ppm], appear in the spectrum of compound *Z*-**2a**.

Thermal relaxation of *Z*-**2a** to *E*-**2a** was investigated at 25 °C in $CDCl_3$, within 45 days in the dark, with the rate constant $k = 1.27 \times 10^{-9}$ s^{-1}.
From the kinetic study, half-live for transition from *Z*-**2a** to *E*-**2a** was : $t_{1/2} \approx$ 6300 days (17.2 years) at 25 °C.

Thermal relaxation of *Z*-**2a** to *E*-**2a** was investigated at 60 °C in $CDCl_3$, within 72 hours in the dark, with the rate constant $k = 4.10 \times 10^{-7}$ s^{-1}.
Half-live for transition from *Z*-**2a** to *E*-**2a** was : $t_{1/2}$ = 19.5 days at 60 °C.

Thermal relaxation of *E*-**2a** to *Z*-**2a** was investigated at 60 °C in $CDCl_3$, within 72 hours in the dark, with the rate constant $k = 2.10 \times 10^{-8}$ s^{-1}.
Half-live for transition from *E*-**2a** to *Z*-**2a** was : $t_{1/2} \approx$ 382 days at 60 °C.

Thermal relaxation of *Z*-**2a** to *E*-**2a** was investigated at 80 °C in toluene-d8, within 72 hours in the dark, with the rate constant $k = 6.2 \times 10^{-7}$ s^{-1}.
Half-live for transition from *E*-**2a** to *Z*-**2a** was : $t_{1/2}$ = 12.9 days at 80 °C.

The NMR spectra were recorded with relaxation times d_1 = 2s. For compound (*Z*)-**2a**, after heating a sample in toluene at 80 °C for 72h, NMR spectra have been recorded with d1 = 2s and d1 = 10s, for comparison purposes (Figure S14, top spectrum).

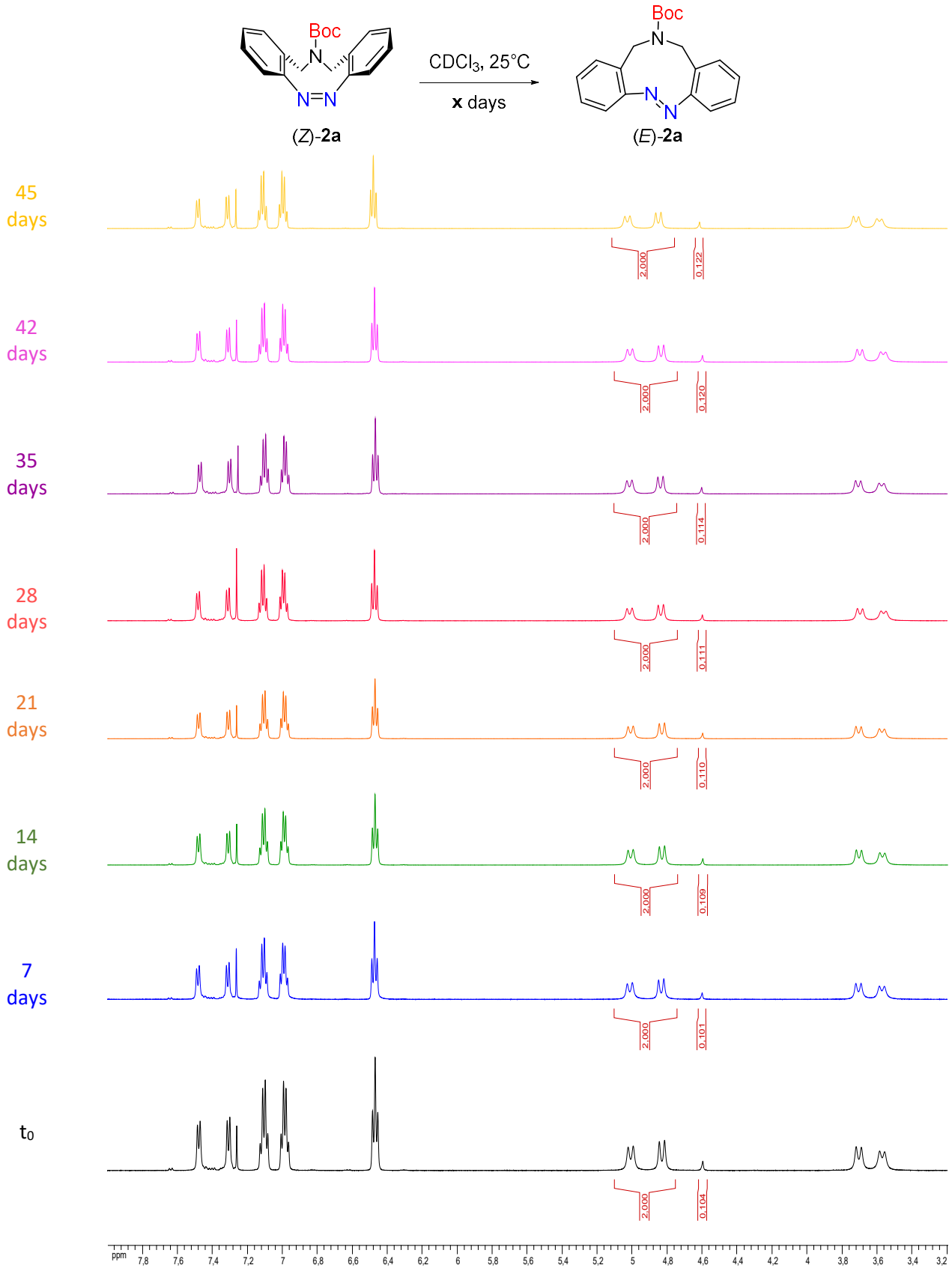

***Figure S11**. Thermal isomerization of (Z)-**2a** followed by ^{1}H NMR experiments, within 45 days at 25 °C in $CDCl_3$ in the dark.*

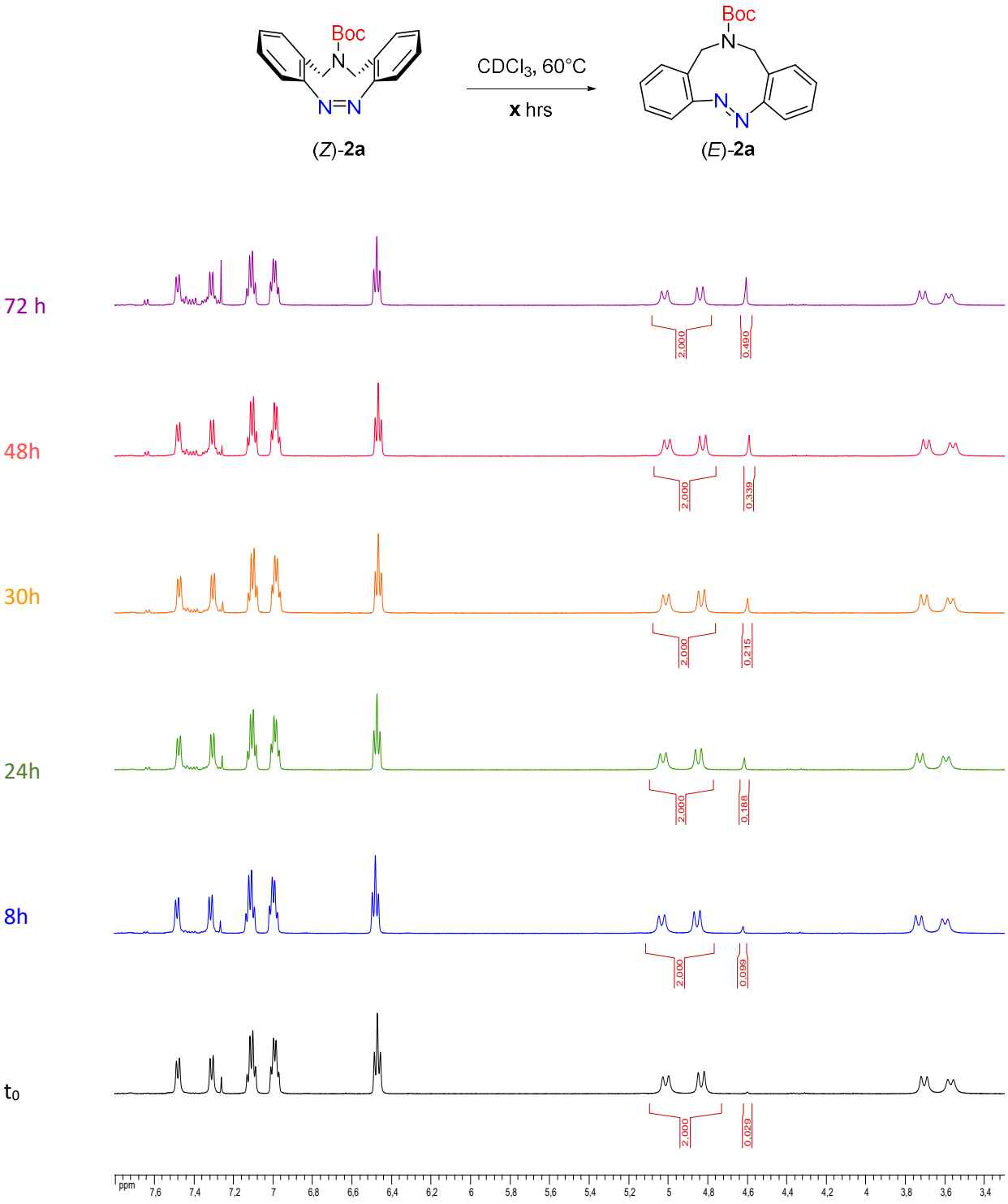

***Figure S12**. Thermal isomerization of (Z)-**2a** followed by ^{1}H NMR experiments, within 72 hours at 60 °C in $CDCl_3$ in the dark.*

Note : a $CDCl_3$ solution of either *E*- or *Z*-**2a** has been charged in an NMR tube and heated in an oil bath at 80°C (Figures S12 and S13). NMR spectra have been recorded at different reaction times. Considering that the boiling point of $CDCl_3$ is 60.9 °C, the effective temperature of the solution should be close to this value.

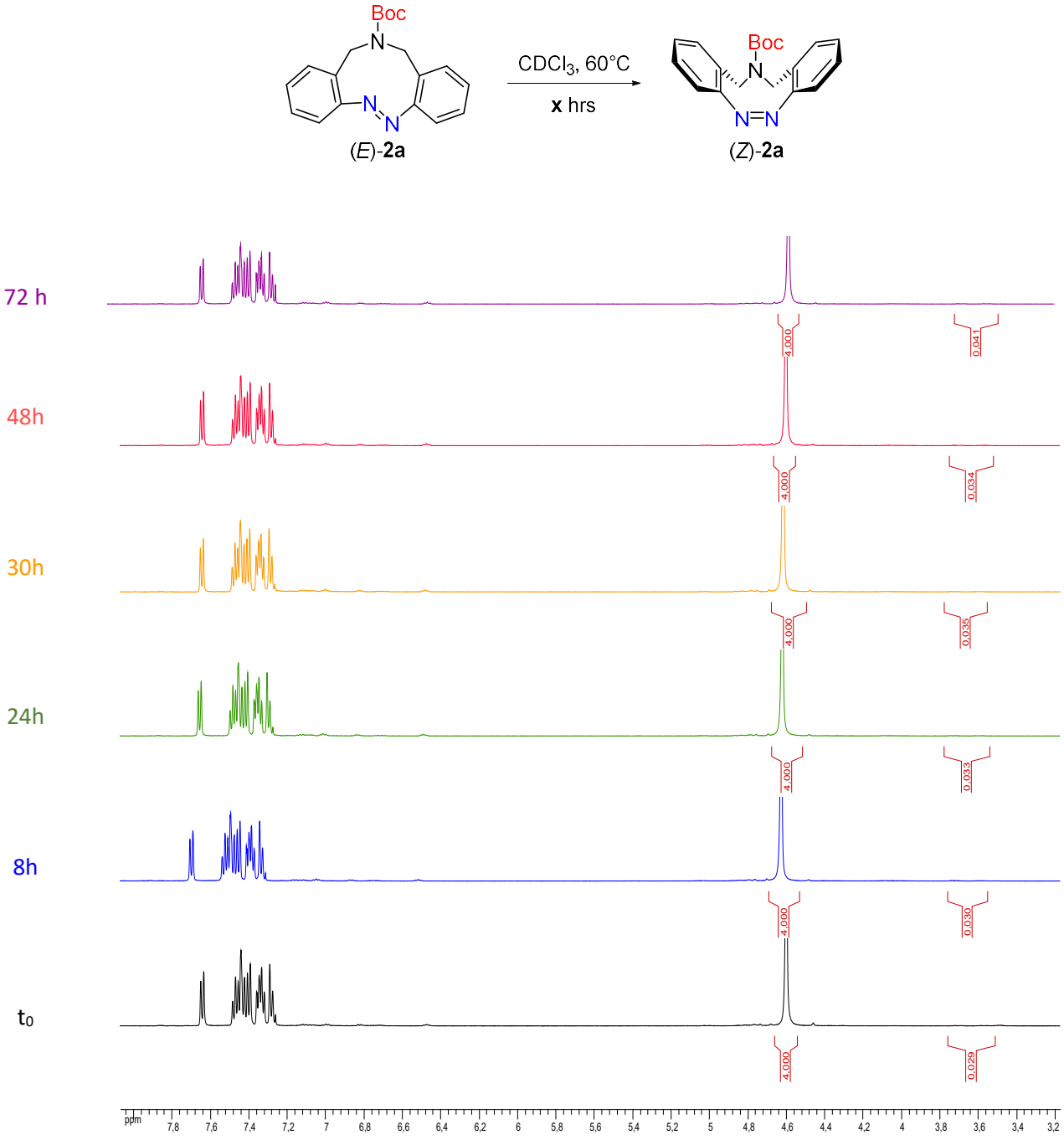

***Figure S13**. Thermal isomerization of (E)-**2a** followed by ^{1}H NMR experiments, within 72 hours at 60 °C in $CDCl_3$ in the dark.*

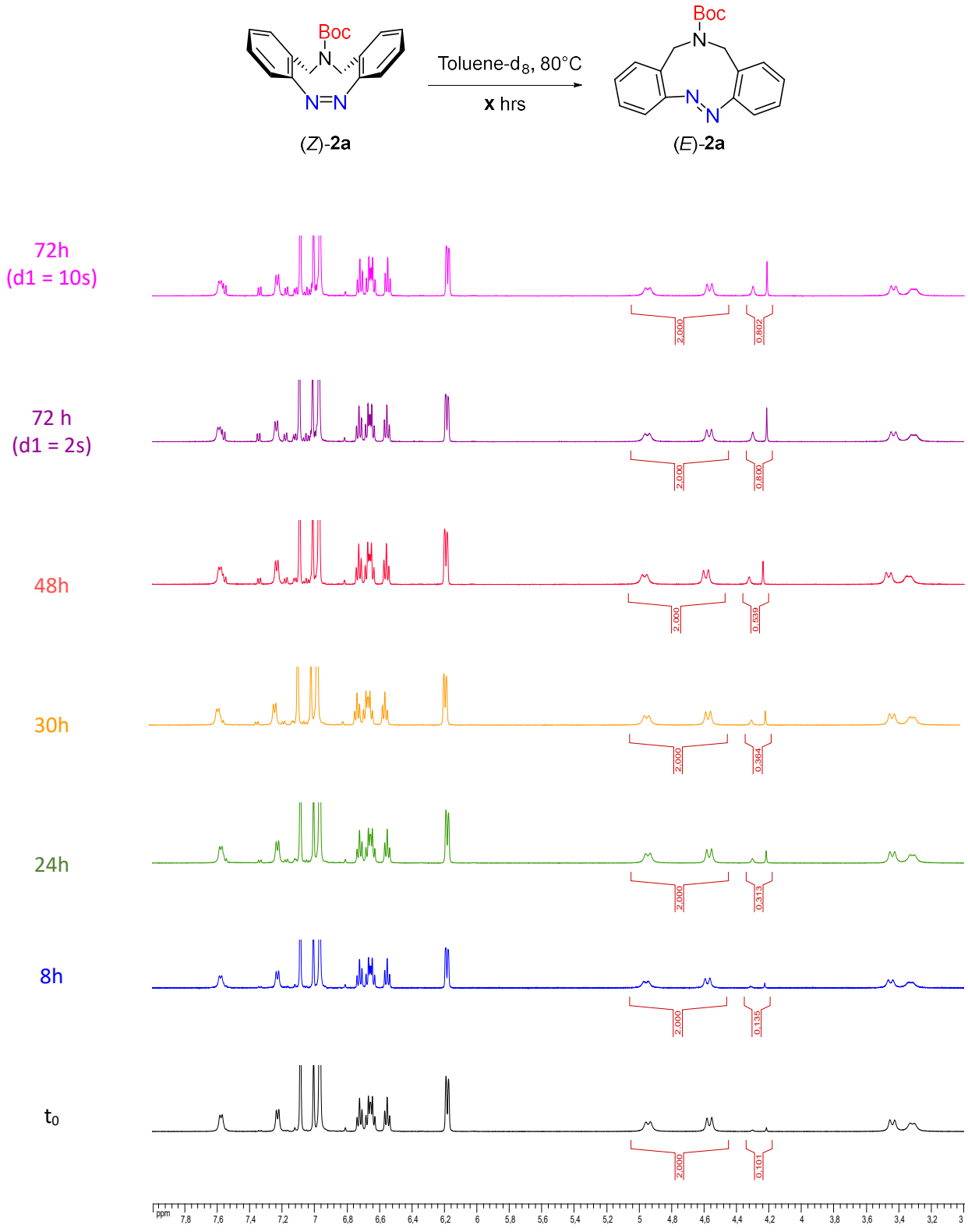

Figure S14. *Thermal isomerization of (Z)-**2a** followed by ^{1}H NMR experiments, within 72 hours at 80 °C in toluene-d8 in the dark. Note: benzylic CH_2 protons of (E)-**2a** in toluene are two singlets [δ 4.20 and 4.30 ppm].*

Time (days)	*E* (%)	*Z* (%)
0	2.5	97.5
7	2.5	97.5
14	2.6	97.4
21	2.7	97.3
28	2.7	97.3
35	2.8	97.2
42	2.9	97.1
45	3.0	97.0

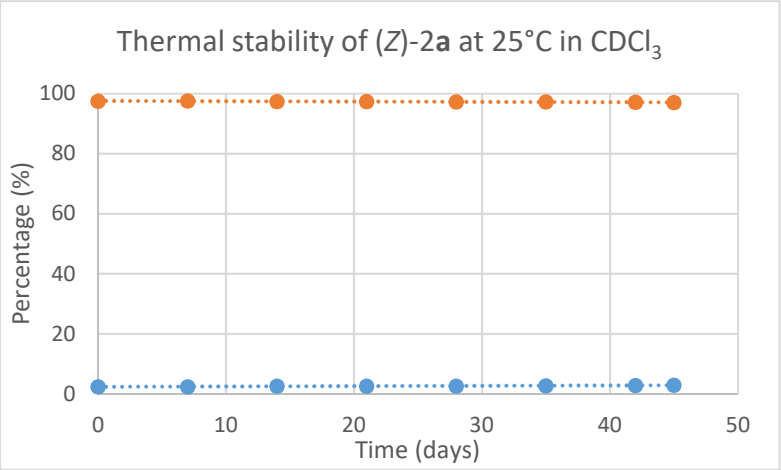

***Figure S15**. Amounts of (Z)-2**a** and (E)-2**a** after 45 days at 25 °C in $CDCl_3$ in the dark.*

Time (h)	*E* (%)	*Z* (%)
0	0.7	99.3
8	2.4	97.6
24	4.5	95.5
30	5.1	94.9
48	7.8	92.2
72	10.9	89.1

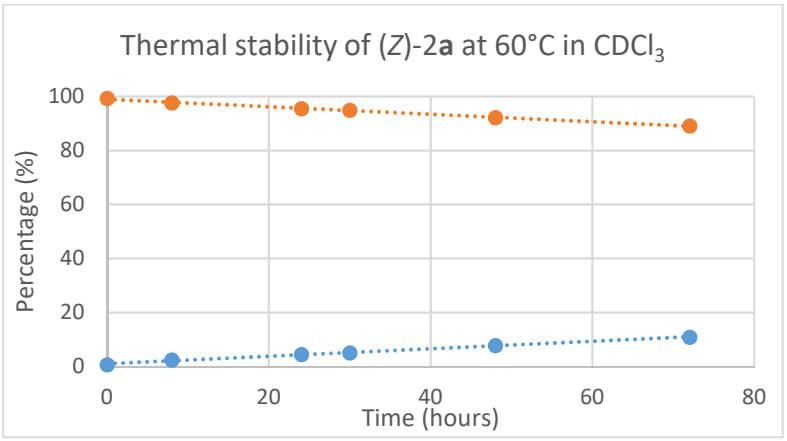

***Figure S16**. Amounts of (Z)-2**a** and (E)-2**a** after 72 hours at 60 °C in $CDCl_3$ in the dark.*

Time (h)	*E* (%)	*Z* (%)
0	98.6	1.4
8	98.5	1.5
24	98.4	1.6
30	98.3	1.7
48	98.3	1.7
72	98.0	2.0

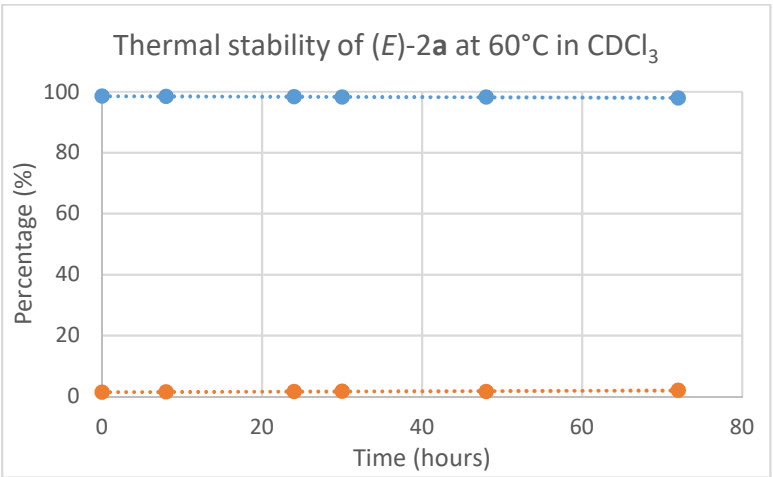

***Figure S17**. Amounts of (E)-2**a** and (Z)-2**a** after 72 hours at 60 °C in $CDCl_3$ in the dark.*

Time (h)	*E* (%)	*Z* (%)
0	2.5	97.5
8	3.3	96.7
24	7.2	92.8
30	8.4	91.6
48	11.9	88.1
72	16.7	83.3
72 (d1=10s)	16.7	83.3

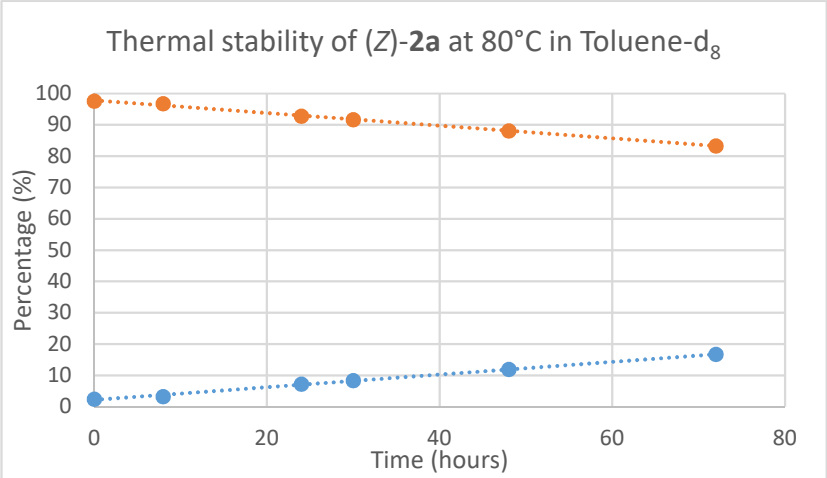

***Figure S18**. Amounts of (Z)-2**a** and (E)-2**a** after 72 hours at 80 °C in toluene-d_8 in the dark.*

VIII. Theoretical studies.

The DFT geometry optimization with a B3LYP functional and a 6-311+G** basis set (figures S11-14) confirmed a planar structure for the *E*-isomer and a bent one for the *Z*-isomer. The bond lengths, angles and dihedrals are gathered in tables S6-9.

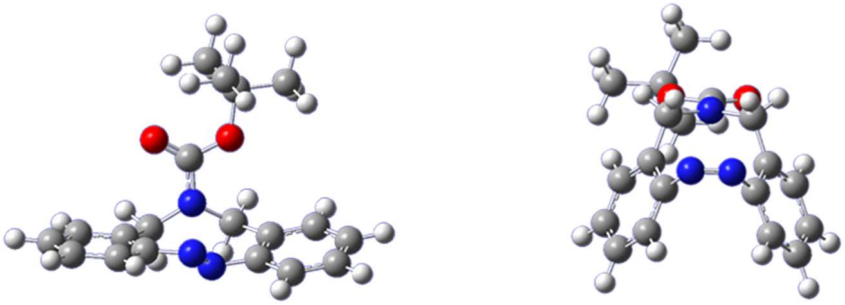

***Figure S19**. Optimized structures (B3LYP/6-311+G**) of the E (left) and Z (right) isomers of **2a**.*

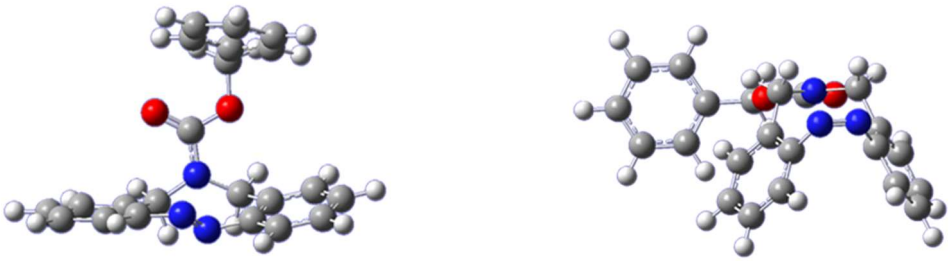

***Figure S20**. Optimized structures (B3LYP/6-311+G**) of the E (left) and Z (right) isomers of **2b**.*

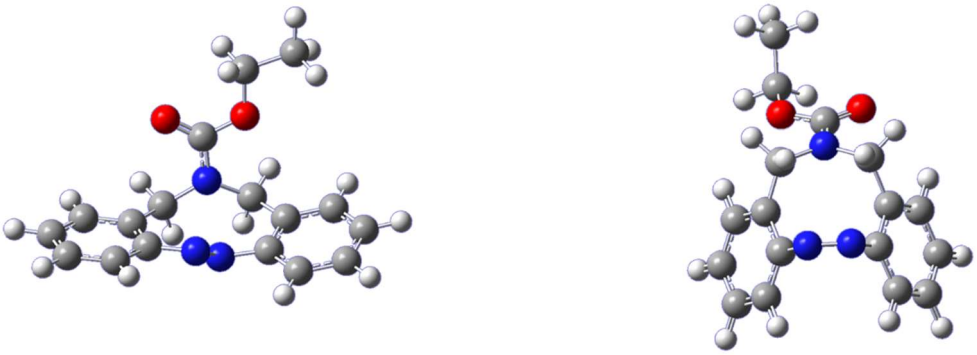

***Figure 21**. Optimized structures (B3LYP/6-311+G**) of the E (left) and Z (right) isomers of **2c**.*

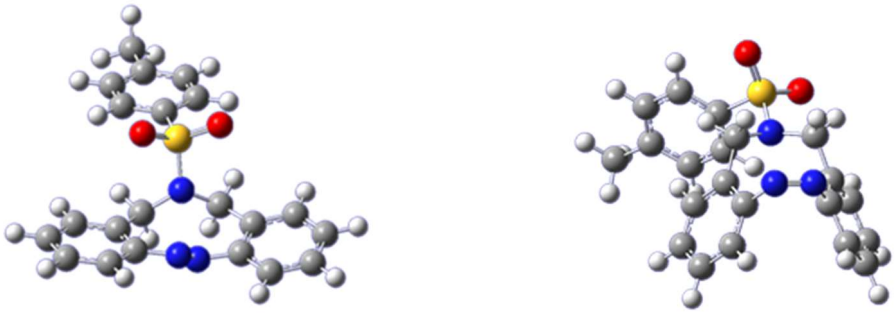

***Figure S22**. Optimized structures (B3LYP/6-311+G**) of the E (left) and Z (right) isomers of **4**.*

A comparison of the bond lengths, angles and dihedrals of the 9-membered ring of the diazocine between the XRD and the optimized DFT structures is reported in tables S6-9. The values are in good agreement, with a maximum discrepancy of 0.096 Å for the bond lengths, 3° for the angles and 6° for the dihedrals.

E-isomer

bond	***1-2***	***2-3***	***3-4***	***4-5***	***5-6***	***6-7***	***7-8***	***8-9***	***9-1***
XRD / Å	1.480	1.528	1.404	1.423	1.254	1.425	1.399	1.428	1.475
DFT / Å	1.475	1.536	1.417	1.422	1.246	1.414	1.405	1.524	1.480

angle	***1-2-3***	***2-3-4***	***3-4-5***	***4-5-6***	***5-6-7***	***6-7-8***	***7-8-9***	***8-9-1***	***9-1-2***
XRD / °	119.5	128.7	120.7	110.6	115.3	112.5	118.3	113.4	119.2
DFT / °	119.6	127.2	121.9	111.6	117.5	111.8	119.7	116.4	120.0

dihedral	***1-2-3-4***	***2-3-4-5***	***3-4-5-6***	***4-5-6-7***	***5-6-7-8***	***6-7-8-9***	***7-8-9-1***	***8-9-1-2***	***9-1-2-3***
XRD / °	-40.6	8.6	-39.3	163.2	-127.0	0.0	48.1	-115.2	122.0
DFT / °	-42.5	5.6	-34.8	163.8	-127.0	-0.4	44.0	-109.1	123.0

Z-isomer

bond	***1-2***	***2-3***	***3-4***	***4-5***	***5-6***	***6-7***	***7-8***	***8-9***	***9-1***
XRD / Å	1.465	1.515	1.392	1.454	1.249	1.456	1.394	1.515	1.461
DFT / Å	1.469	1.521	1.401	1.45	1.239	1.45	1.401	1.521	1.471

angle	***1-2-3***	***2-3-4***	***3-4-5***	***4-5-6***	***5-6-7***	***6-7-8***	***7-8-9***	***8-9-1***	***9-1-2***
XRD / °	112.6	121.2	120.3	119.7	118.6	120.2	121.9	115.5	118.0
DFT / °	114.8	122.0	120.3	121.3	121.4	120.5	122.0	114.7	118.7

dihedral	***1-2-3-4***	***2-3-4-5***	***3-4-5-6***	***4-5-6-7***	***5-6-7-8***	***6-7-8-9***	***7-8-9-1***	***8-9-1-2***	***9-1-2-3***
XRD / °	-90.8	-7.4	95.9	1.9	-83.4	1.4	97	-81	80.4
DFT / °	-90.9	-5.5	89.1	0.6	-90.8	6.2	89.4	-83.9	84.7

Table S6*. Comparison between the optimized (B3LYP/6-311+G**) and XRD structure of the bond lengths and of the angles of the 9-membered ring of the diazocine, in the E and Z isomers of* ***2a****.*

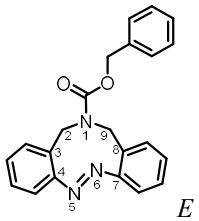

E

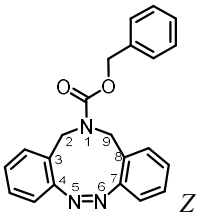

Z

bond	***1-2***	***2-3***	***3-4***	***4-5***	***5-6***	***6-7***	***7-8***	***8-9***	***9-1***
***E* / Å**	1.477	1.535	1.417	1.422	1.246	1.413	1.405	1.524	1.482
***Z* / Å**	1.471	1.520	1.401	1.450	1.239	1.450	1.401	1.521	1.473

angle	***1-2-3***	***2-3-4***	***3-4-5***	***4-5-6***	***5-6-7***	***6-7-8***	***7-8-9***	***8-9-1***	***9-1-2***
***E* / °**	119.5	127.3	122.0	111.6	117.6	111.7	119.7	116.4	120.1
***Z* / °**	114.6	122.0	120.3	121.4	121.5	120.5	121.9	114.6	119.0

dihedral	***1-2-3-4***	***2-3-4-5***	***3-4-5-6***	***4-5-6-7***	***5-6-7-8***	***6-7-8-9***	***7-8-9-1***	***8-9-1-2***	***9-1-2-3***
***E* / °**	-42.8	5.8	-34.4	163.7	-127.4	-0.6	44.2	-109.1	122.9
***Z* / °**	-90.1	-5.9	89.6	0.3	-90.6	6.3	89.3	-84.4	84.8

Table S7*. Calculated (B3LYP/6-311+G**) bond lengths and angles of the 9-membered ring of the diazocine, in the E and Z isomers of* ***2b****.*

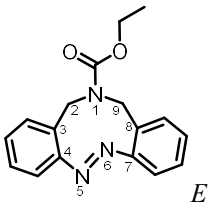

E

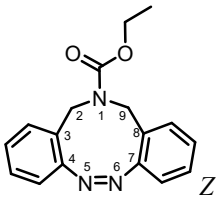

Z

bond	***1-2***	***2-3***	***3-4***	***4-5***	***5-6***	***6-7***	***7-8***	***8-9***	***9-1***
***E* / Å**	1.476	1.536	1.417	1.422	1.246	1.414	1.405	1.524	1.481
***Z* / Å**	1.472	1.521	1.402	1.450	1.239	1.450	1.401	1.520	1.470

angle	***1-2-3***	***2-3-4***	***3-4-5***	***4-5-6***	***5-6-7***	***6-7-8***	***7-8-9***	***8-9-1***	***9-1-2***
***E* / °**	119.56	127.24	121.93	111.64	117.56	111.73	119.72	116.40	120.16
***Z* / °**	114.67	121.90	120.41	121.51	121.46	120.31	121.99	114.62	118.94

dihedral	***1-2-3-4***	***2-3-4-5***	***3-4-5-6***	***4-5-6-7***	***5-6-7-8***	***6-7-8-9***	***7-8-9-1***	***8-9-1-2***	***9-1-2-3***
***E* / °**	-42.77	5.77	-34.53	163.74	-127.34	-0.48	44.07	-109.04	122.98
***Z* / °**	89.42	6.34	-90.37	0.18	89.93	-6.16	-89.81	84.85	-84.73

Table S8. *Calculated (B3LYP/6-311+G**) bond lengths and angles of the 9-membered ring of the diazocine, in the E and Z isomers of* ***2c****.*

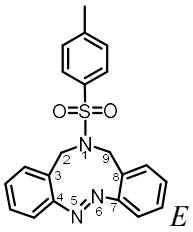

E

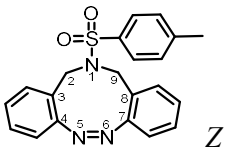

Z

bond	***1-2***	***2-3***	***3-4***	***4-5***	***5-6***	***6-7***	***7-8***	***8-9***	***9-1***
***E* / Å**	1.489	1.531	1.418	1.421	1.246	1.413	1.406	1.521	1.492
***Z* / Å**	1.487	1.517	1.400	1.450	1.241	1.450	1.402	1.516	1.487

angle	***1-2-3***	***2-3-4***	***3-4-5***	***4-5-6***	***5-6-7***	***6-7-8***	***7-8-9***	***8-9-1***	***9-1-2***
***E* / °**	118.4	126.7	122.2	111.7	117.7	111.7	119.6	115.1	118.8
***Z* / °**	113.5	122.4	120.9	120.7	120.6	120.4	122.1	113.1	115.8

dihedral	***1-2-3-4***	***2-3-4-5***	***3-4-5-6***	***4-5-6-7***	***5-6-7-8***	***6-7-8-9***	***7-8-9-1***	***8-9-1-2***	***9-1-2-3***
***E* / °**	-44.8	6.4	-33.1	163.4	-128.5	-0.8	44.3	-110.3	125.8
***Z* / °**	93.6	2.5	-89.2	0.9	87.1	-1.8	-96.2	84.8	-83.3

Table S9. *Calculated (B3LYP/6-311+G**) bond lengths and angles of the 9-membered ring of the diazocine, in the E and Z isomers of* ***4****.*

The TD-DFT calculations were conducted starting from the optimized geometries (6-311+G**) with either the B3LYP or the CAM-B3LYP functionals and with the 6-311+G** basis set.

Isomer	*ΔE (2a) / kcal mol^{-1}*	*ΔE (2b) / kcal mol^{-1}*	*ΔE (2c) / kcal mol^{-1}*	*ΔE 4 / kcal mol^{-1}*
E (ground state)	0	0	0	0
Z (ground state)	3.3	2.6	3.63	4.4
E:Z population	99.6 : 0.4	98.7 : 1.3	99.8 :0.2	99.9 : 0.1

***Table S10**. Energies of the two isomers in the ground and excited states calculated with the B3LYP functional.*

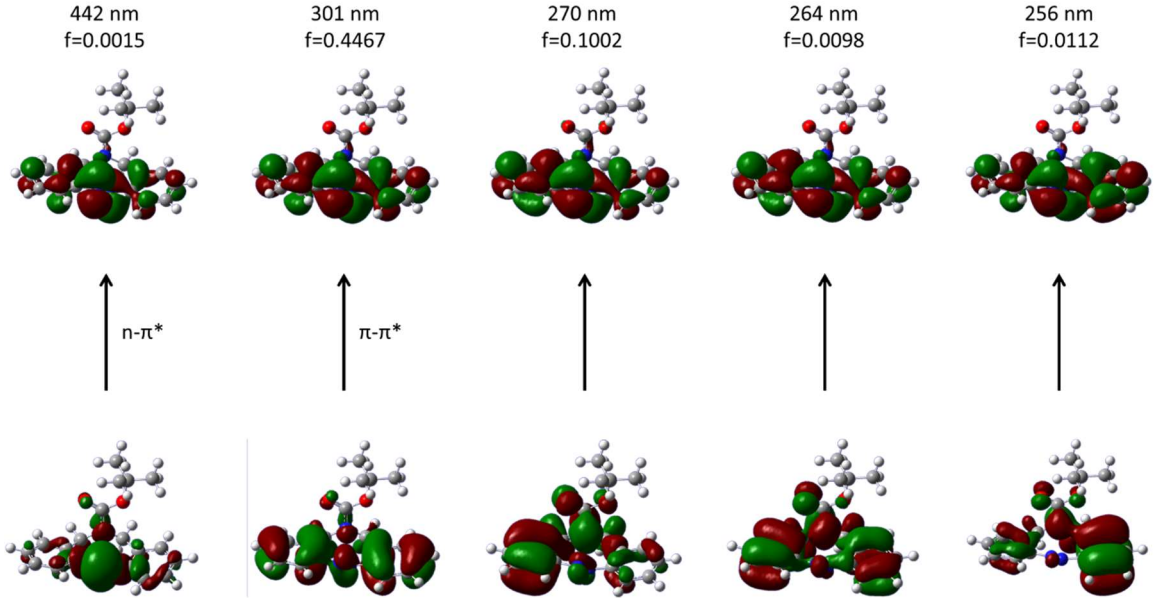

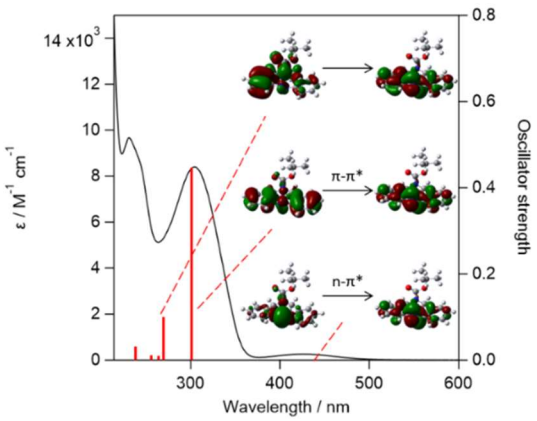

***Figure S23**. NTO for the first electronic transitions of E-**2a** (top) and NTO orbitals, calculated transitions (red) and experimental spectra (black) of E-**2a** in CH_3CN (bottom).*

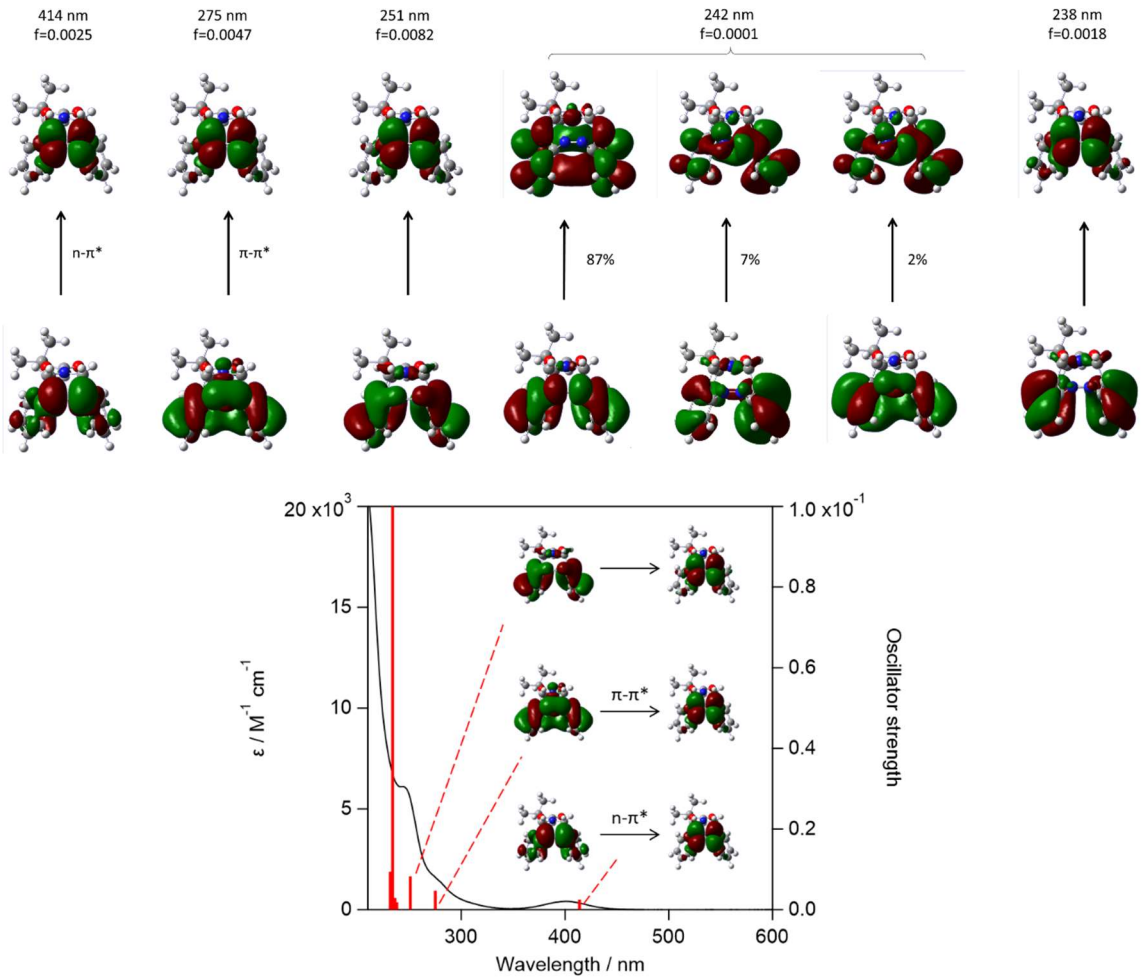

Figure S24*. NTO for the first electronic transitions of Z-**2a** (top) and NTO orbitals, calculated transitions (red) and experimental spectra (black) of Z-**2a** in CH_3CN (bottom).*

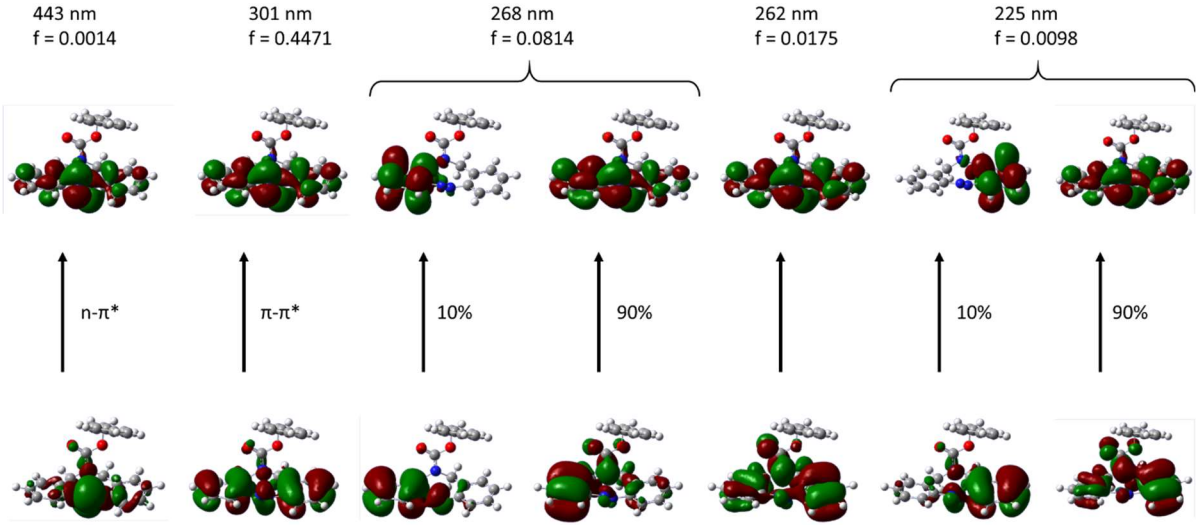

Figure S25. *NTO for the first electronic transitions of E-**2b**.*

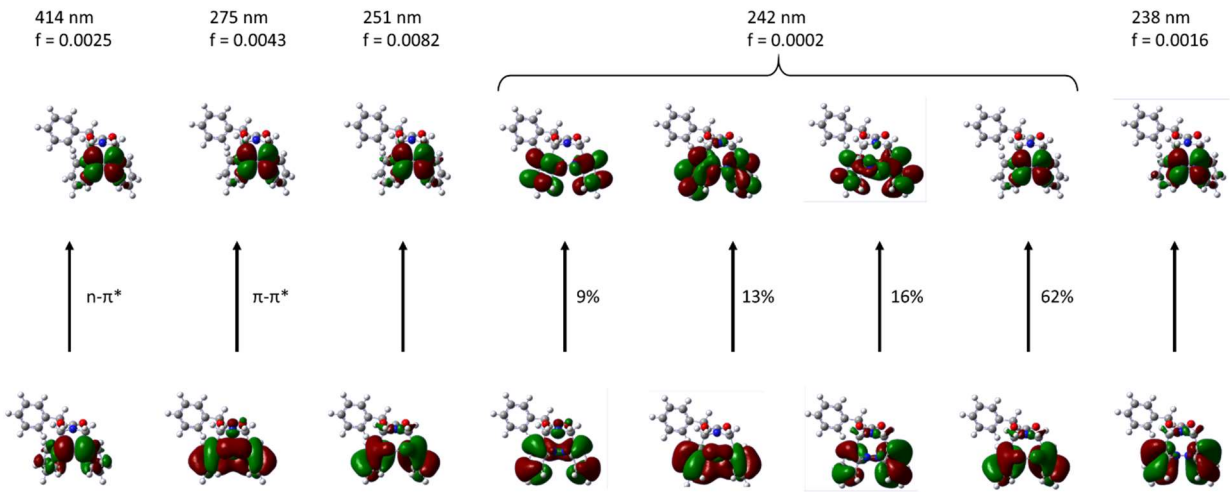

***Figure S26**. NTO for the first electronic transitions of Z-**2b**.*

The results of the NTO analyses are reported in figure S15-21. In the *E* isomer, the first two transitions display a clear n-π* and π-π* character, respectively, and the remainder transitions at high energies partially involve the carbonyl of the protecting group; in the *Z*-isomer, the first two transitions maintain the n-π* and π-π* character, but in the remainder transitions the contribution from the protecting group is almost negligible.

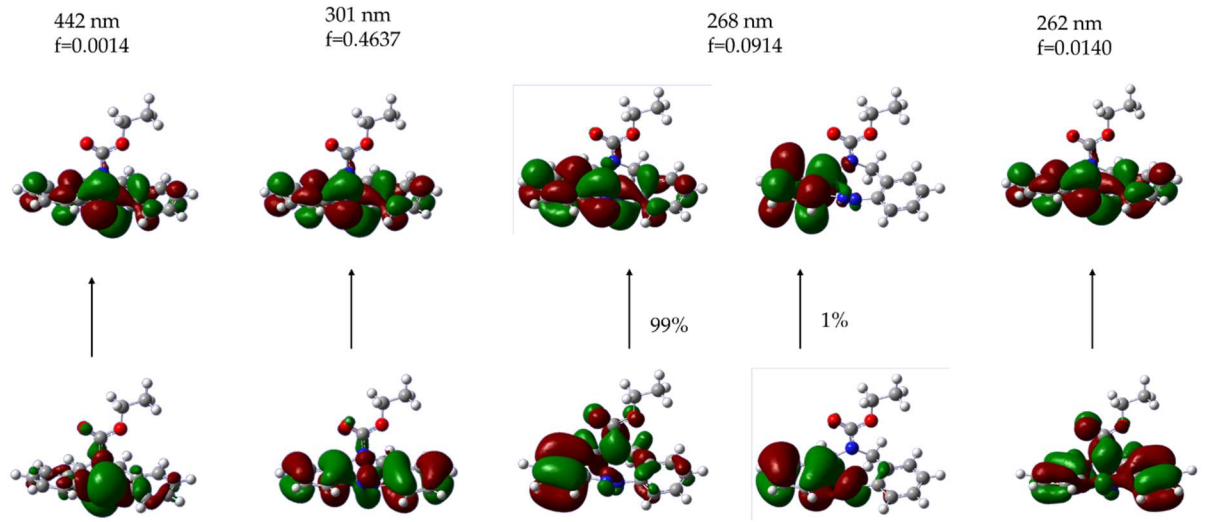

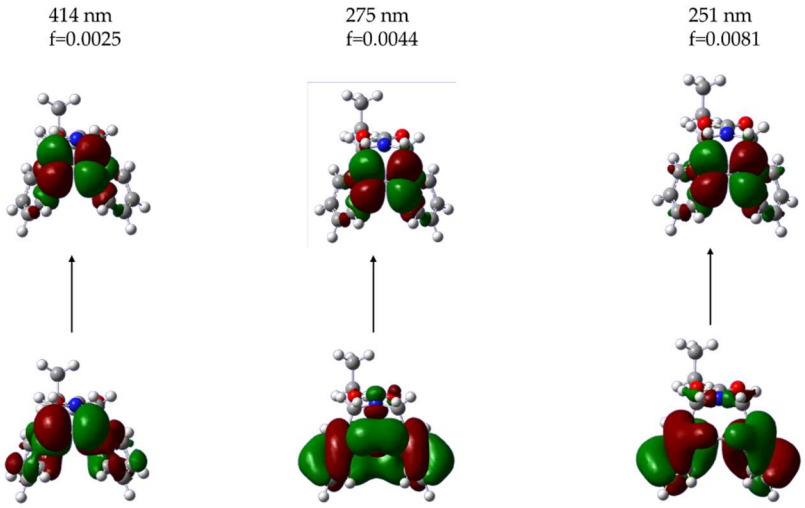

***Figure S27**. NTO orbitals for the first transitions in the E (top) and Z isomer of **2c**.*

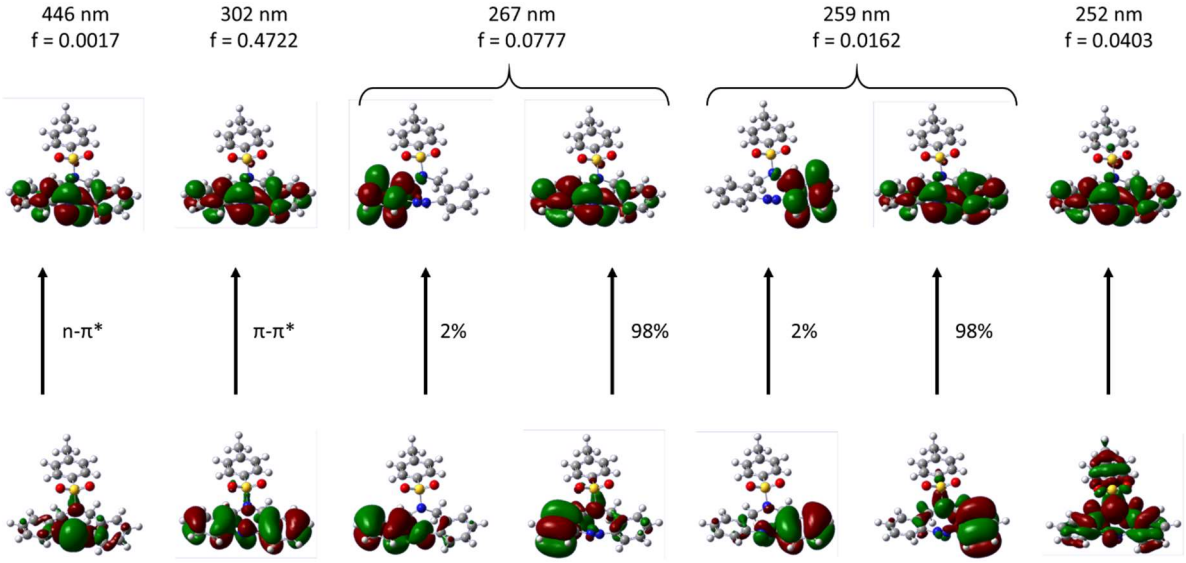

***Figure S28**. NTO for the first electronic transitions of E-**4**.*

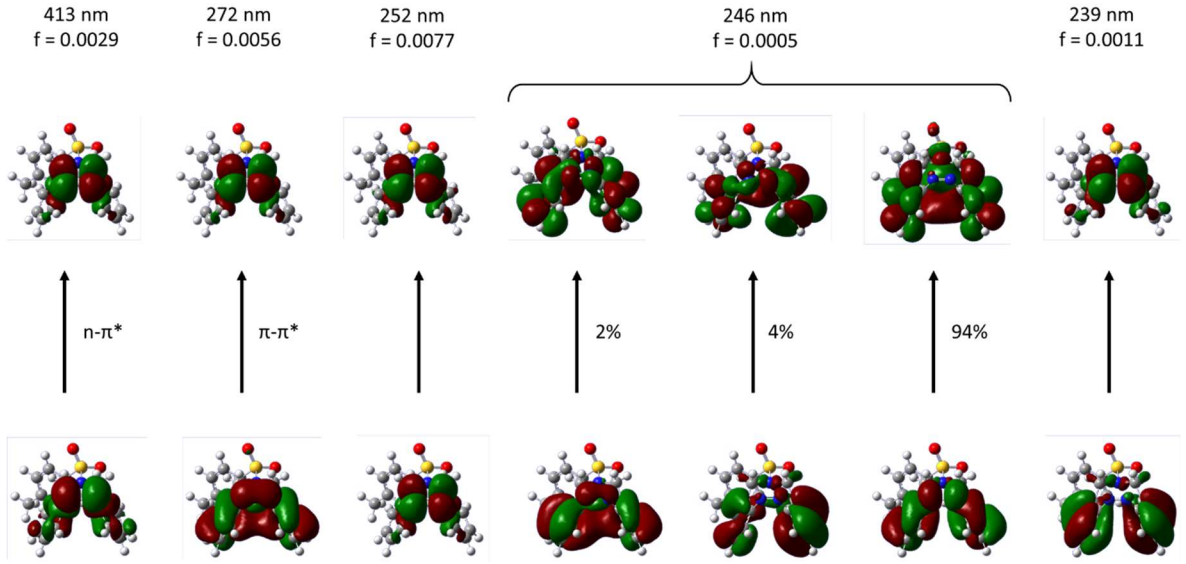

***Figure S29**. NTO for the first electronic transitions of Z-**4**.*

IX. Comparison of photochromic properties of some diazocine and diazonine cyclic azobenzenes.

Name	**diazocine**[9]	**O-diazocine**[10]	**S-diazocine**[10]	**NFmoc-diazocine**[11]
Structure	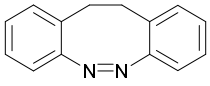	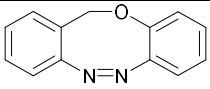	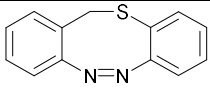	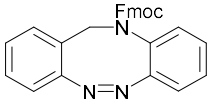
Stable isomer	*Z*-isomer	*Z*-isomer	*Z*-isomer	*Z*-isomer
% PSS	385 nm PSS: 92% *E* 520 nm PSS: 99% *Z*	385 nm PSS: 80% *E* 520 nm PSS: 99% *Z*	405 nm PSS: 70% *E* 520 nm PSS: 99% *Z*	405 nm PSS: 80% *E* 520-590 nm PSS: >99% *Z*
$t_{1/2}$	*E*-*Z* $t_{1/2}$ = 4.5 h at 28.5 °C	*E*-*Z* $t_{1/2}$ = 89 s at 20 °C	*E*-*Z* $t_{1/2}$ = 3.5 d at 27 °C	*E*-*Z* $t_{1/2}$ = 42 min at 25 °C

Name	**thiadiazonines**[12]	**diazonines**[13]	**triazonine 2a** *(this work)*
Structure	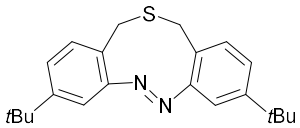	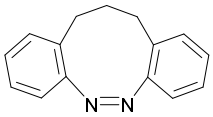	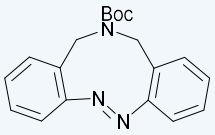
Stable isomer	*E*-isomer	*Z*-isomer	*E*-isomer
% PSS	366 nm PSS: *nd* 466 nm PSS: 30% *E*	390 nm PSS: 86% *E* 520 nm (*PSS not determined*)	334 nm PSS: 93% *Z* 405 nm PSS: 86% *E*
$t_{1/2}$	*Z*-*E* $t_{1/2}$ = 30 min at 25 °C	*not determined*	*Z*-*E* $t_{1/2}$ ≈ 6301 days at 25 °C *Z*-*E* $t_{1/2}$ = 19.5 days at 60 °C

[9] R. Siewertsen, H. Neumann, B. Buchheim-Stehn, R. Herges, C. Naether, F. Renth and F. Temps, *J. Am. Chem. Soc.*, 2009, **131**, 15594.
[10] M. Hammerich, C. Schuett, C. Staehler, P. Lentes, F. Roehricht, R. Hoeppner and R. Herges, *J. Am. Chem. Soc.*, 2016, **138**, 13111.
[11] P. Lentes, E. Stadler, F. Roehricht, A. Brahms, J. Groebner, F. D. Soennichsen, G. Gescheidt and R. Herges, *J. Am. Chem. Soc.*, 2019, **141**, 13592.
[12] M. Saha, S. Ghosh and S. Bandyopadhyay, *New J. Chem.*, 2018, **42**, 10784.
[13] M. S. Maier, K. Hüll, M. Reynders, B. S. Matsuura, P. Leippe, T. Ko, L. Schäffer and D. Trauner, *J. Am. Chem. Soc.*, 2019, **141**, 17295.